IAC-08-A3.3.A1

MISSION AND NAVIGATION DESIGN FOR THE 2009 MARS SCIENCE LABORATORY MISSION

Louis A. D'Amario
Principal Member Engineering Staff
Jet Propulsion Laboratory, California Institute of Technology, Pasadena, California (USA) 91109
Louis.A.Damario@jpl.nasa.gov

NASA's Mars Science Laboratory mission will launch the next mobile science laboratory to Mars in the fall of 2009 with arrival at Mars occurring in the summer of 2010. A heat shield, parachute, and rocket-powered descent stage, including a sky crane, will be used to land the rover safely on the surface of Mars. The direction of the atmospheric entry vehicle lift vector will be controlled by a hypersonic entry guidance algorithm to compensate for entry trajectory errors and counteract atmospheric and aerodynamic dispersions. The key challenges for mission design are (1) develop a launch/arrival strategy that provides communications coverage during the Entry, Descent, and Landing phase either from an X-band direct-to-Earth link or from a Ultra High Frequency link to the Mars Reconnaissance Orbiter for landing latitudes between 30 deg North and 30 deg South, while satisfying mission constraints on Earth departure energy and Mars atmospheric entry speed, and (2) generate Earth-departure targets for the Atlas V-541 launch vehicle for the specified launch/arrival strategy. The launch/arrival strategy employs a 30-day baseline launch period and a 27-day extended launch period with varying arrival dates at Mars. The key challenges for navigation design are (1) deliver the spacecraft to the atmospheric entry interface point (Mars radius of 3522.2 km) with an inertial entry flight path angle error of ±0.20 deg (3σ), (2) provide knowledge of the entry state vector accurate to ±2.8 km (3σ) in position and ±2.0 m/s (3σ) in velocity for initializing the entry guidance algorithm, and (3) ensure a 99% probability of successful delivery at Mars with respect to available cruise stage propellant. Orbit determination is accomplished via ground processing of multiple complimentary radiometric data types: Doppler, range, and Delta-Differential One-way Ranging (a Very Long Baseline Interferometry measurement). The navigation strategy makes use of up to five interplanetary trajectory correction maneuvers to achieve entry targeting requirements. The requirements for cruise propellant usage and atmospheric entry targeting and knowledge are met with ample margins.

INTRODUCTION

The Mars Science Laboratory (MSL) mission will deliver a mobile science laboratory rover to the surface of Mars during the 2009 Mars launch opportunity. The overall scientific goal of the mission is to explore and quantitatively assess a local region on Mars' surface as a potential habitat for life, past or present. The MSL spacecraft will be launched in September-November 2009 from the Eastern Test Range at Cape Canaveral Air Force Station in Florida on an Atlas V 541 launch vehicle and will arrive at Mars in July-September 2010.

The flight system consists of an Earth-Mars cruise stage and atmospheric entry vehicle. The entry vehicle consists of a heatshield, backshell, descent stage (including sky crane), and the rover. The rover carries a suite of 10 science instruments within the categories of remote sensing, in-situ, analytical, and environmental (Ref. 1). The rover is powered by a Multi-Mission Radioisotope Thermoelectric Generator (MMRTG).

During the critical ~6 min Entry, Descent, and Landing (EDL) phase, the entry system will transmit telemetry to the Mars Reconnaissance Orbiter (MRO) and the Mars Odyssey Orbiter (ODY), both of which will be flying overhead, and also directly to Earth. The requirements for EDL telecom coverage via relay through MRO and ODY and direct-to-Earth (DTE) are significant drivers for mission design.

Following brief overviews of the mission and spacecraft in the next two sections, the remainder of the paper will address mission and navigation design requirements and results.

MISSION

Launch

The MSL spacecraft is scheduled to be launched during the 2009 launch opportunity to Mars. The launch vehicle is an Atlas V 541* consisting of a liquid oxygen / kerosene Common Core Booster (CCB) first stage and a liquid oxygen / liquid hydrogen Centaur upper stage. The first Centaur burn establishes the 165 km x 287 km, 28.9 deg inclination parking orbit, and the second Centaur burn injects the spacecraft onto the interplanetary transfer trajectory. The baseline 30-day launch period with MRO and DTE EDL coverage extends from 15 September through 14 October 2009. An extended launch period of up to 27 additional launch days extends from 15 October through

* For the Atlas nomenclature, "5" denotes five strap-on solid rocket boosters, "4" denotes a 4 m payload fairing, and "1" denotes a single-engine Centaur upper stage.

10 November 2009. The launch window on any given day during the launch period has a duration of up to 120 min, depending on launch vehicle performance and the required injection energy. The launch vehicle injection targets are specified as hyperbolic injection energy per unit mass (C_3), declination of the launch asymptote (DLA), and right ascension of the launch asymptote (RLA) at the targeting interface point (TIP), defined as 5 min after spacecraft separation from the Centaur. The injected spacecraft mass is ~4100 kg, corresponding to a maximum C_3 of ~19.4 km^2/s^2. The maximum required C_3 is 17.1 km^2/s^2 for the baseline launch period and 17.3 km^2/s^2 for the extended launch period. Excess launch vehicle performance determines the duration of the daily launch window.

Interplanetary Cruise

A plot of the interplanetary trajectory for the open of the launch period is shown in Figure 1 (Ref. 2). The duration of interplanetary cruise is ~10 months. The Earth range at arrival is between 1.88 and 2.17 AU, depending on launch date. Detailed interplanetary trajectory characteristics can also be found in Ref. 2.

During interplanetary cruise, up to six Trajectory Correction Maneuvers (TCMs) are performed to control the trajectory and adjust the atmospheric entry aimpoint, where the entry interface point is defined to be at a Mars radius of 3522.2 km. The TCM profile is shown in Table 1. In addition, periodic attitude maintenance turns are performed to provide adequate power and telecom margins, and checkouts and calibrations of various spacecraft systems are carried out. The spacecraft is spin-stabilized at 2 rpm during cruise.

The final 45 days prior to arrival at Mars are referred to as the approach phase. During approach, the amount of navigation tracking data increases

TCM	Location*	Description
TCM-1	L + 15 days	Correct injection errors; remove part of injection bias required for planetary protection.
TCM-2	L + 120 days	Correct TCM-1 errors; remove part of injection bias required for planetary protection.
TCM-3	E - 60 days	Correct TCM-2 errors; target to desired atmospheric entry aimpoint.
TCM-4	E - 8 days	Correct TCM-3 errors.
TCM-5	E - 2 days	Correct TCM-4 errors.
TCM-5X	E - 1 day	Contingency maneuver for failure to execute TCM-5.
TCM-6	E - 7 hrs	Contingency maneuver: final opportunity to correct entry aimpoint.
*Time measured from Launch (L) or Entry (E).		

Table 1: TCM Profile.

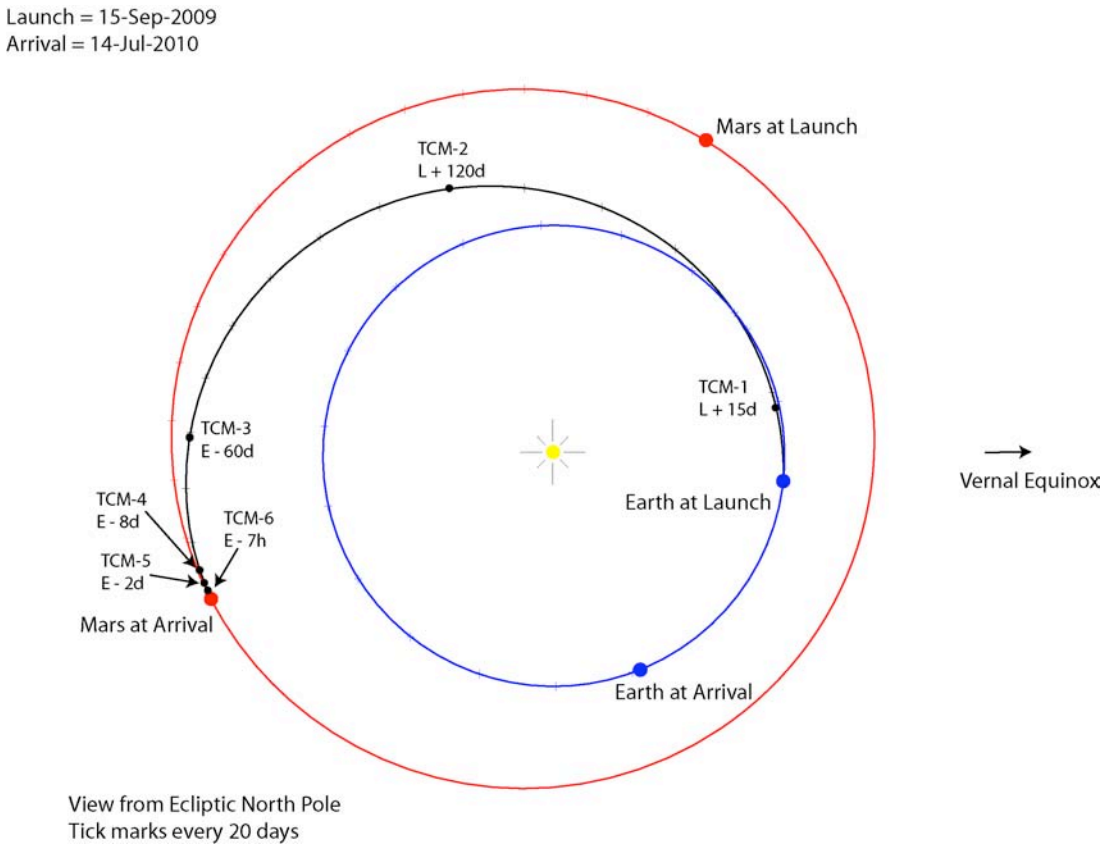

Figure 1: Interplanetary Trajectory for Launch on 15 September 2009.

significantly, and spacecraft activities are focused on approach navigation, specifically TCMs 4 and 5 (and TCMs 5X or 6, if necessary), as well as preparations for EDL, which include initializing the onboard EDL flight software with the latest estimate of the atmospheric entry state vector.

Entry, Descent, and Landing (EDL)

MSL is the first Mars mission to employ a guided (as opposed to ballistic) hypersonic entry in order to reduce landing dispersions[†]. Prior to atmospheric entry, two cruise balance masses are ejected to establish a center-of-mass offset. This causes the entry vehicle to have a non-zero angle of attack that provides a lift force. During the hypersonic entry period, an onboard guidance algorithm controls the direction of the lift vector (by rolling or "banking" the entry vehicle) in order to compensate for entry state errors and counteract atmospheric and aerodynamic dispersions. This enables MSL to achieve landing dispersions of ~12 km (99%) measured radially from the target landing point.

Prior to atmospheric entry (E) a final update to the entry state vector (if necessary) is uplinked to the spacecraft as late as E – 2 hrs to initialize the onboard guidance algorithm. About three minutes prior to cruise stage separation, the cruise stage Heat Rejection System (HRS) is vented. Cruise stage separation itself occurs at E – 10 min. The entry vehicle is then despun and turned to the desired entry attitude, and the cruise balance masses are ejected. Atmospheric entry is defined to occur at a Mars radius of 3522.2 km (~150 km altitude).

During the hypersonic deceleration period, the onboard guidance algorithm uses knowledge of entry state vector errors and sensed accelerations to apply a lift force to null out entry trajectory errors and counteract atmospheric and aerodynamic dispersions to fly to the target landing point. At ~E + 4 min at a speed of about Mach 2.0 (450 m/s) and an altitude of ~10 km, the supersonic parachute is deployed, and shortly thereafter, the heatshield is separated. At ~E + 5 min at a (mostly vertical) speed of ~100 m/s and an altitude of ~1.9 km, the descent stage, carrying the rover, is separated from the backshell. The descent stage fires its rocket motors to slow to a vertical speed of ~0.75 m/s at an altitude of ~20 m. The 900 kg rover is then deployed from the descent stage and lowered to the surface using a bridle mechanism referred to as the "sky crane". Touchdown occurs at ~E + 6 min. The descent stage then cuts the bridle and executes a "flyaway" maneuver to impact the surface at a safe distance from the rover.

During EDL, communications coverage is provided via a direct-to-Earth (DTE) X-band link to the NASA Deep Space Network (DSN) and via relay through MRO and ODY using a UHF link from MSL to the orbiters. EDL coverage is also possible via relay through the Mars Express MEX) orbiter, although this option is not currently part of the baseline mission plan.

Figure 2 shows the locations of the seven current MSL candidate landing sites, along with the landing sites for the Viking, Mars Pathfinder, and Mars Exploration Rover (MER) missions. Note that all the MSL candidate landing sites are within a latitude range from 30N to 30S. As this paper was being prepared, Gale Crater was added to the list of candidate landing sites, and S. Meridiani replaced the nearby N. Meridiani landing site. The most important effect on mission and navigation design from adding these sites is that the total range of landing longitudes is now significantly greater. This change is an issue only with respect to the ΔV required for landing site retargeting after launch and is addressed later in this paper.

Surface

The surface phase of the mission has a nominal duration of one Martian year, which is 669 Sols or 687 Earth days. One Sol is one Martian day or 24 hrs 37 min. During this time, the rover will drive to targets of interest to conduct science investigations that focus on acquisition and analysis of soil samples. During surface operations, communications with the rover and data return are accomplished via a DTE link and via relay through MRO and ODY. The science plan for the mission is described in detail in Ref. 1.

SPACECRAFT

Figure 3 shows an expanded view of the MSL flight system, and Figure 4 shows the flight system in cruise configuration.

The MSL flight system consists of an interplanetary cruise stage and an atmospheric entry vehicle, which is comprised of the heatshield, backshell, descent stage (including sky crane) and rover. The mass allocation for the entire flight system, including propellant, is 4100 kg. During interplanetary cruise, the spacecraft is spin-stabilized at a nominal spin rate of 2 rpm. During the EDL phase, the entry vehicle is three-axis controlled.

The cruise stage includes solar panels, the propulsion system, which includes two propellant tanks and two thruster clusters, the Attitude Control System (ACS), which includes a star scanner, Inertial Measurement Unit (IMU), and Sun sensors, and two antennas for X-band communications with Earth: a Low Gain Antenna (LGA) and a Medium Gain Antenna (MGA).

Cruise Stage Propulsion System

The cruise stage propulsion system (based on MER design) consists of two propellant tanks, feed lines, a

[†] The Viking landers used a simple open-loop guidance scheme solely to maintain constant lift throughout EDL.

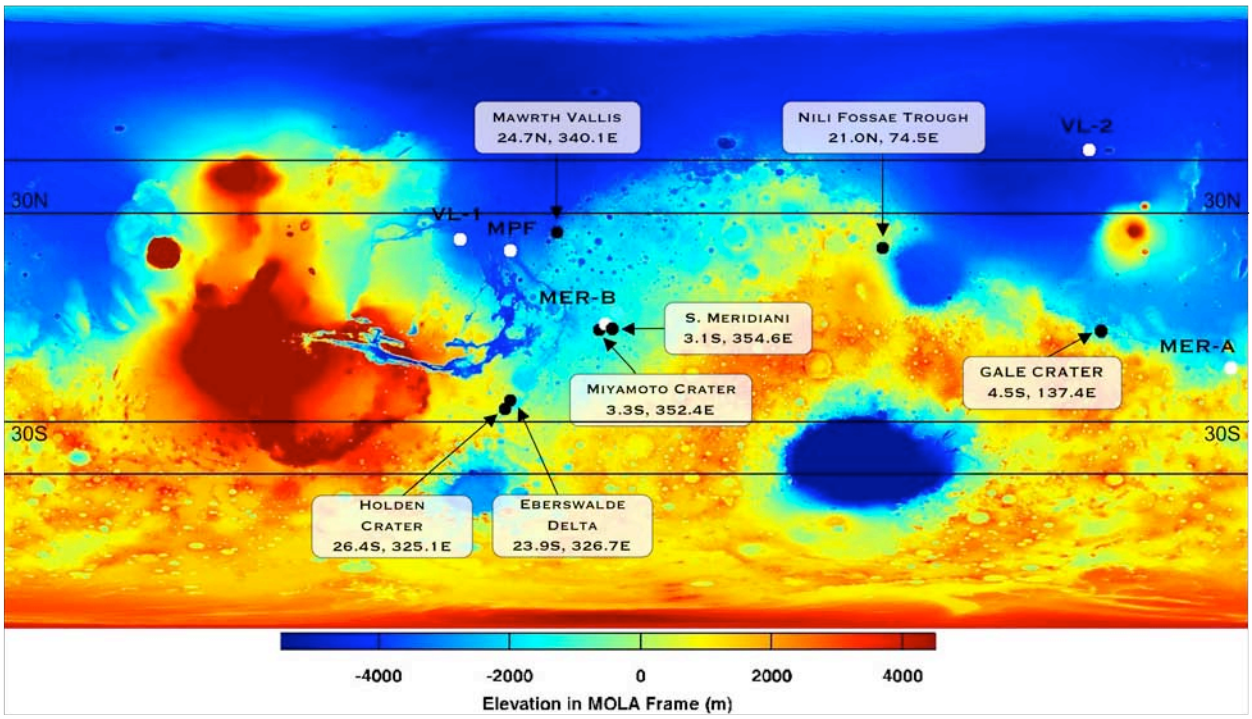

Figure 2: Candidate MSL Landing Sites.

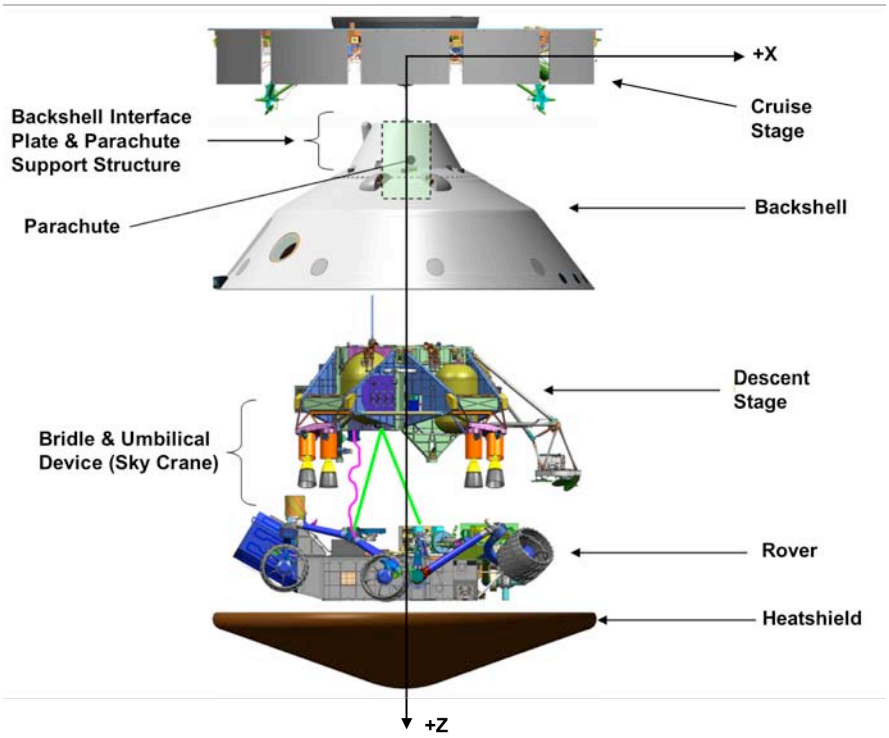

Figure 3: MSL Flight System – Expanded View.

propellant filter, two latch valves, and eight ~5 N thrusters in two clusters of four thrusters each. The thrusters are used for spin-rate control, attitude control, and TCMs during cruise. The total usable propellant load is 70 kg.

The thruster clusters are diametrically opposed and located in a plane normal to the Z-axis along a line rotated 45 deg from the X axis toward the Y axis. Two of the thrusters in each cluster ("axial" thrusters) are

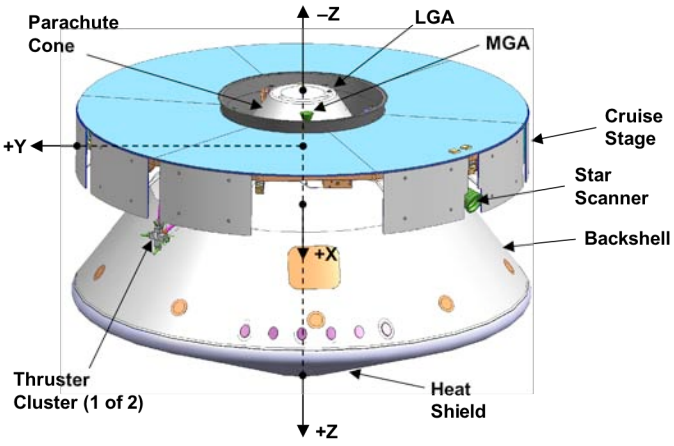

Figure 4: MSL Flight System – Cruise Configuration.

canted 40 deg toward the +Z and –Z directions. The other two thrusters in each cluster ("lateral" thrusters) are canted 40 deg away from the line connecting the two thruster clusters in a plane normal to the Z-axis.

An axial burn imparts ΔV in the +Z or –Z direction and is accomplished by firing pairs of axial thrusters continuously for a specified time. A lateral burn imparts ΔV in a direction approximately normal to the Z-axis and is accomplished by firing all four thrusters in each cluster for 5 s (60 deg burn arc) at the appropriate orientation during each spacecraft revolution, thereby providing two 5 s lateral "pulses" per revolution).

Spacecraft attitude maneuvers (turns) and spin-rate control are accomplished by pulse-mode firing of coupled thruster pairs. Nominally, there is no ΔV imparted to the spacecraft from thruster firings for spacecraft turns. Thruster misalignments and thrust imbalances, however, can cause a small residual ΔV. Therefore, an ACS/NAV characterization (consisting of a pre-determined sequence of spacecraft turns) is performed following TCM-1 to characterize the level of residual ΔV, which is an important error source modeled in the orbit determination process.

The I_{sp} values for axial and lateral burns for TCMs are 212.4 s and 221.8 s. These are average values to reflect blowdown effects during interplanetary cruise, and they have also been adjusted to account for thruster plume impingement losses of 6% for axial burns and 1% for lateral burns.

Telecom System

The MSL telecommunications subsystem uses X-band for direct-to-Earth (DTE) communications during all mission phases and a UHF system during EDL and also during the surface mission for relay communications through the MRO and ODY orbiters.

The X-band system provides both X-band uplink and downlink. Downlink can be coherent or non-coherent with the uplink. The following X-band antennas are used (see Figure 5):

- One cruise stage MGA for interplanetary cruise
- One parachute-cone-mounted LGA (PLGA) for interplanetary cruise and part of EDL
- One backshell-mounted tilted LGA (TLGA) for EDL
- A HGA and LGA pair on the Rover for surface operations

Two redundant UHF transceivers in the rover support the following antennas (see Figure 5):

- One parachute-cone-mounted UHF antenna (PUHF) for EDL.
- One descent stage antenna (DUHF) for EDL
- One rover-mounted UHF antenna (RUHF) for surface operations

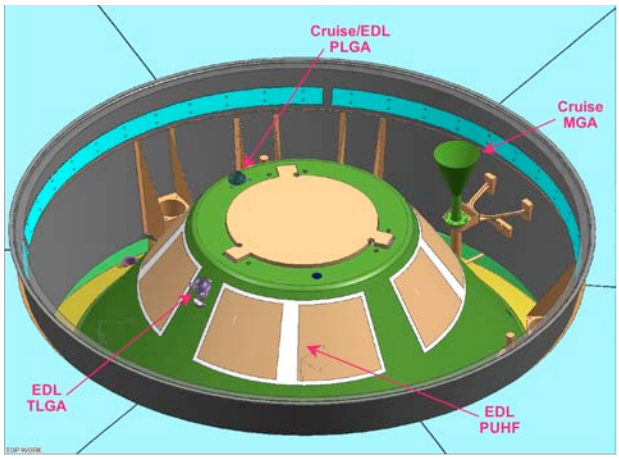

Figure 5: Cruise Stage and Backshell Antennas.

REQUIREMENTS

The key driving requirements for mission and navigation design are listed below.

Launch/Arrival Strategy and EDL Coverage

- The launch period shall be at least 24 consecutive days beginning on 15 September 2009 with a launch window duration of at least 30 min.
- The launch/arrival strategy shall allow for pre-launch selection of EDL coverage via either an X-band DTE link or a UHF link to an orbiting asset from atmospheric entry through landing plus one minute.
- The launch/arrival strategy shall accommodate landing site latitudes between 30N and 30S.
- The atmosphere-relative entry speed shall be between 5.3 km/s and 5.6 km/s.

Launch Trajectory Design

- Launch shall occur during daylight.

- The time from launch to eclipse exit or spacecraft separation, whichever is later, shall be less than 65 min.

Planetary Protection

- Launch vehicle injection targets shall be biased away from Mars to ensure that the probability of Mars impact by the launch vehicle upper stage is less than 1.0×10^{-4}.
- The cruise TCM strategy shall ensure that the probability of non-nominal impact of Mars due to spacecraft failure during cruise is less than 1.0×10^{-2}.

TCM ΔV and Propellant

- The 99% probability value for propellant required for TCMs and attitude/spin maintenance shall be less than the available propellant.
- The design for cruise TCMs shall be constrained to allow continuous X-band communications during all maneuvers.

Atmospheric Entry Delivery/Knowledge Accuracies

- The entry vehicle shall be delivered to the specified atmospheric entry conditions with an inertial entry flight path angle (EFPA) error less than ±0.20 deg (3σ).
- The EDL flight software shall be initialized with a state vector at an epoch at E – 9 min with accuracies of 2.8 km (3σ) in position and 2.0 m/s (3σ) in velocity.

MISSION DESIGN

The topics addressed in this section are launch/arrival strategy, launch period characteristics, EDL coverage characteristics, and launch trajectory characteristics.

Launch/Arrival Strategy

Requirements, Constraints, and Assumptions

The launch/arrival strategy consists of selection of the *launch period*, defined as the set of contiguous launch dates that provide opportunities for injection onto interplanetary transfer trajectories to Mars, and an *arrival date* for each launch date, such that all mission requirements and constraints are met (or nearly met).

The primary considerations for the launch/arrival strategy are launch vehicle performance, spacecraft mass, constraints caused by the EDL systems design, requirements for EDL communications coverage, and the range of landing latitudes.

Launch vehicle performance and spacecraft mass together determine the maximum achievable launch energy (C_3).

The EDL systems design levies constraints directly on atmosphere-relative entry speed and indirectly on Mars arrival date. The upper limit for entry speed (5.6 km/s) is dictated by the capability of the thermal protection system used for the heatshield. The arrival date determines the season on Mars at arrival (measured by a quantity called Ls[‡]), which has a large effect on atmospheric density and the probability of dust storms. Both of these factors affect the maximum achievable landing site altitude and the number of candidate landing sites.

EDL communications coverage, either via a DTE link or via a relay through MRO, depends heavily on Mars arrival geometry and EDL trajectory geometry, which are functions of launch date, arrival date, and landing site latitude. EDL trajectory geometry is also a function of the inertial entry flight path angle (EFPA), which is selected based on EDL performance considerations. The nominal EFPA value is –15.5 deg, with a range of possible values between –14.0 deg and –15.5 deg. The sensitivity of EDL coverage to EFPA must be taken into account when designing the launch/arrival strategy.

EDL coverage through MRO is heavily dependent on the orientation of MRO's orbit. MRO is in a low-altitude, sun-synchronous, frozen orbit with the ascending node nominally at a Local Mean Solar Time (LMST) of 3:00 PM.

The factors mentioned above result in the following list of requirements, constraints, and assumptions for determining the launch/arrival strategy:

- $C_3 < 19.4$ km^2/s^2.
- Atmosphere-relative entry speed < 5.6 km/s.
- Ls at arrival < ~125 deg.
- Provide DTE EDL coverage from separation to entry for landing latitudes between 30N and 30S.
- Provide MRO and DTE EDL coverage from entry to landing plus one minute for landing latitudes between 30N and 30S.
- MRO antenna angle (angle between MSL anti-velocity vector and direction to MRO) < 120 deg between entry and landing + 1 min.
- DTE antenna angle (angle between MSL anti-velocity vector and direction to Earth) < 75 deg between entry and landing + 1 min.
- Elevation of MRO or Earth > 10 deg at landing and landing plus + 1 min.
- MSL must not be occulted by Mars as seen from MRO between entry and landing + 1 min

[‡] Ls is the longitude of the Sun as viewed from Mars measured eastward from the vernal equinox of Mars. Ls is effectively a measure of the position of Mars in its orbit. Ls = 0 deg is the start of northern spring (southern fall), Ls = 90 deg is the start of northern summer (southern winter), Ls = 180 deg is the start of northern fall (southern spring), and Ls = 270 deg is the start of northern winter (southern summer).

- Nominal EFPA is –15.5 deg (inertial)
- MRO ascending node is nominally at 3:00 PM (LMST).

It should be pointed out that MRO and ODY EDL coverage are considered significantly more valuable than DTE EDL coverage. The primary reason is that the relay link to MRO or ODY provides a high telemetry data rate (up to 32 kbps), whereas the DTE link provides only "tones" that confirm that particular events have completed onboard the spacecraft. The added advantage of ODY coverage is that ODY can relay data from MSL to Earth in real time (similar to what was done for the Mars Phoenix lander). The launch/arrival strategy has been designed to provide complete EDL coverage from MRO and ODY while accepting less than complete DTE EDL coverage, if necessary.

Launch/Arrival Strategy

The resulting launch/arrival strategy is illustrated in Figure 6, with launch date on the horizontal axis and arrival date on the vertical axis. The figure shows the baseline and extended launch periods as well as contours of C_3, DLA, and inertial entry speed. (Inertial entry speed is shown, because atmosphere-relative entry speed is a function of landing latitude and, to a lesser extent, EFPA; for latitudes between 30N and 30S, relative entry speed is 150 to 250 m/s lower than inertial entry speed.) Ls values are displayed along the right side of the figure. The 30-day baseline launch period extends from 15 September through 14 October 2009 and uses six different arrival dates between 14 July and 1 August 2010. The 27-day extended launch period extends from 15 October through 10 November 2009 and has nearly continually varying arrival dates between 4 August and 5 September 2010.

The baseline and extended launch periods were developed at two different times. Initially, there was only a baseline launch period. The extended launch period was added later in order to provide additional launch opportunities to offer relief in the event of a several week delay in assembly and testing of the complex MSL spacecraft. For the design of the extended launch period, certain requirements and constraints were relaxed, and some assumptions were changed (described below), in order to make it possible to add a significant number of additional launch opportunities.

The approach used for the baseline launch period (see Figure 6) was to find an initial constant arrival date such that on the first launch date for that arrival date, the MRO antenna angle is at its upper limit (120 deg), and on the last day, the entry speed reaches its upper

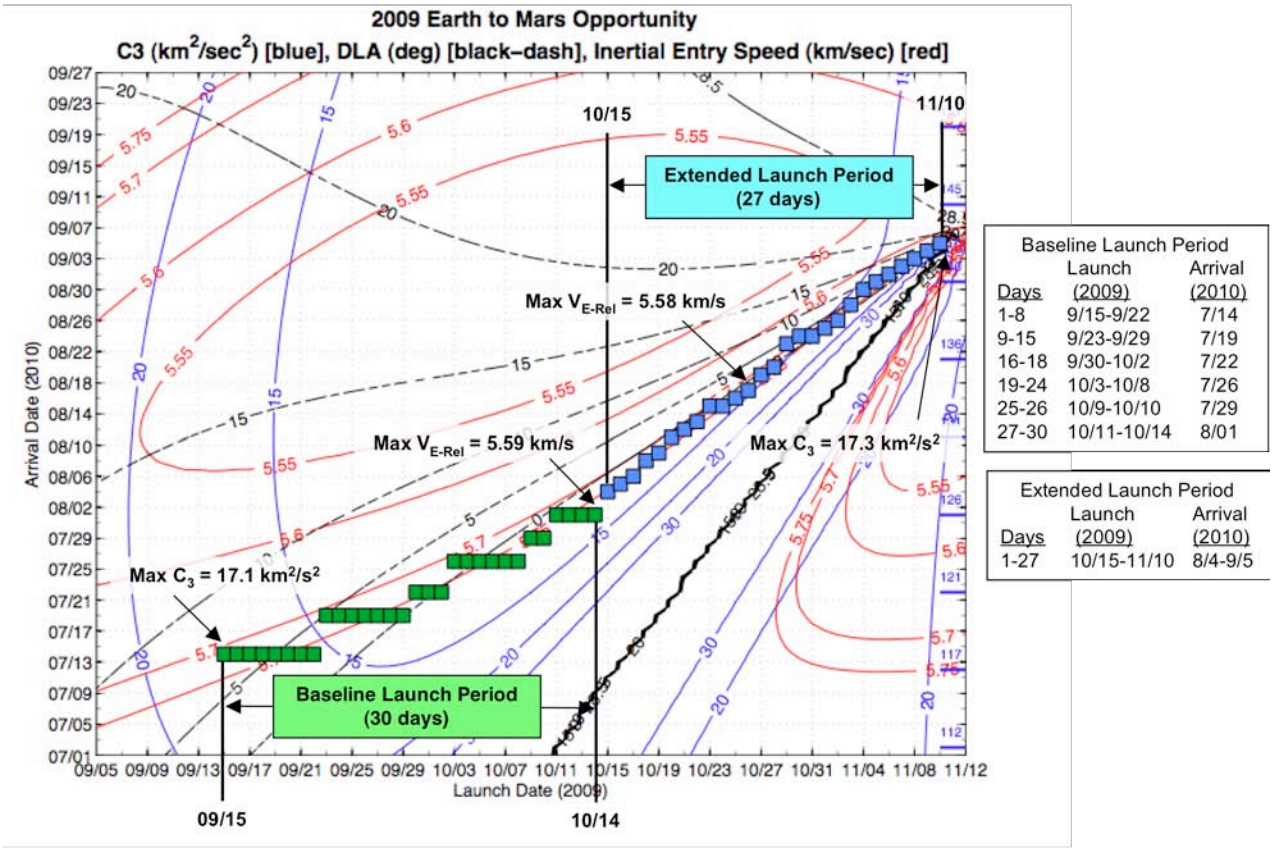

Figure 6: Launch/Arrival Strategy.

limit (5.6 km/s). The arrival date is moved later in steps and the process is repeated. In evaluating EDL coverage, it was assumed that the MRO orbit node was fixed at 3:00 PM, and the effects on EDL coverage constraints of varying the landing latitude between 30N and 30S were accounted for.

For the extended launch period, perhaps the most significant change is that it was assumed that the MRO orbit node could be moved from the nominal value of 3:00 PM, and that the node could be different for different launch dates. The requirement for DTE EDL coverage was waived; however, DTE coverage does still exist. Lastly, the upper limit on Ls (~125 deg) was allowed to be violated. However, in order to keep Ls as low as possible (i.e., keep arrival dates as early as possible), the arrival dates were allowed to vary continually – i.e. a different arrival date could be selected for each launch date. Keeping Ls as low as possible minimizes the degradation to EDL landing altitude capability from adverse atmospheric conditions at later arrival dates (as described above) and the resulting loss of candidate landing sites.

The approach used for the extended launch period (see Figure 6) was to use launch date / arrival date combinations that essentially track along the contour corresponding to an atmospheric entry speed of 5.6 km/s. In evaluating EDL coverage, the MRO orbit node was changed in a stepwise manner in order to satisfy EDL coverage constraints, and the effects on the EDL coverage constraints of varying the landing latitude between 30N and 30S were accounted for.

The desire to have real-time ODY EDL coverage became an issue after both the baseline and extended launch periods were designed. Thus, ODY coverage characteristics are constrained by the launch/arrival strategy developed originally for MRO coverage. Similar to MRO, ODY is in a low-altitude, sun-synchronous, frozen orbit. At the time of MSL arrival at Mars, ODY is expected to have a descending node at 3:00 PM, and this is the value used for analyzing ODY coverage in the baseline launch period. As for MRO, it was assumed that the ODY orbit node could be varied in the extended launch period.

Launch Period Characteristics

The characteristics of the baseline and extended launch periods are shown in Tables 2 and 3. The tables include launch date, arrival date, Ls, launch vehicle injection targets (C_3, DLA, and RLA), and the atmosphere-relative entry speed at the most northerly and southerly candidate landing sites, as well as at a near-equatorial landing site (to illustrate variations with landing latitude).

For the baseline launch period, the maximum C_3 occurs at the open of the launch period, whereas for the extended launch period, the maximum C_3 occurs at the end of the launch period. Based on current Atlas V 541 performance, the maximum achievable C_3 for a 4100 kg payload (the MSL mass allocation) is ~19.4 km^2/s^2. Excess launch vehicle performance is utilized to provide a finite-duration launch window on any given launch day, up to a maximum duration of 2 hrs (selected to bound required launch vehicle trajectory analyses). The maximum DLA magnitude for all launch days in the baseline and extended launch periods is 17.9 deg. Therefore, the standard Atlas V parking orbit with a 28.9 deg inclination will be used. Over the range of landing latitudes for the candidate landing sites, the atmosphere-relative entry speeds are consistently less than the upper limit of 5.6 km/s.

EDL Coverage Characteristics

Mean Anomaly Range for MRO or ODY

For any launch date and landing site, there is a range of mean anomalies for MRO or ODY for which EDL coverage constraints can be satisfied. Initially, this mean anomaly range is determined from the constraints on antenna angle at entry and elevation at landing plus one minute. Nominally, the orbiter may be phased in its orbit anywhere over this range of mean anomalies – for example, to optimize EDL coverage for a particular time period or event. However, there are two factors (described below) that reduce the range of possible mean anomalies.

First, for certain launch days and landing site latitudes, MSL is occulted by Mars as seen from MRO or ODY for some period of time between entry and landing + 1 min. When this situation occurs, the mean anomaly range is reduced to eliminate the occultations in order to provide uninterrupted EDL coverage from entry to landing + 1 min. Secondly, the accuracy with which MRO and ODY can control orbital phasing is ±30 s or ~±1.6 deg for a orbit period of ~2 hr. To account for this uncertainty, the lower and upper bounds of the mean anomaly range are both reduced by 1.6 deg.

In some cases, either there is no resulting mean anomaly range that provides uninterrupted EDL coverage from entry to landing + 1 min or the mean anomaly range is less than 3.2 deg (i.e., twice the phasing control uncertainty). This situation occurs at the most northerly landing latitudes (i.e., Mawrth and Nili landing sites) for the last several days of the baseline launch period.

For these launch days, an exception was made to the assumption that the orbit node for MRO and ODY was fixed at 3:00 PM, and the orbit node was moved to 2:30 PM to provide full EDL coverage.

				Launch Vehicle Injection Targets*			Atmosphere-Relative Entry Speed (km/s)		
Launch Day	Launch Date	Arrival Date	Ls (deg)	C_3 (km^2/sec^2)	DLA (deg)	RLA (deg)	Mawrth (24.88 N)	Meridiani (1.48 N)	Holden (26.37 S)
1	15-Sep-2009	14-Jul-2010	118.1	17.092	7.136	121.707	5.493	5.468	5.496
2	16-Sep-2009		118.1	16.737	6.675	121.526	5.499	5.475	5.503
3	17-Sep-2009		118.1	16.400	6.166	121.285	5.506	5.482	5.511
4	18-Sep-2009		118.1	16.084	5.624	120.997	5.514	5.490	5.519
5	19-Sep-2009		118.1	15.791	5.049	120.663	5.522	5.498	5.527
6	20-Sep-2009		118.1	15.524	4.438	120.290	5.530	5.506	5.536
7	21-Sep-2009		118.1	15.283	3.786	119.881	5.539	5.516	5.545
8	22-Sep-2009		118.1	15.070	3.088	119.437	5.548	5.525	5.555
9	23-Sep-2009	19-Jul-2010	120.5	14.343	5.163	119.408	5.489	5.465	5.495
10	24-Sep-2009		120.5	14.146	4.550	118.920	5.496	5.473	5.504
11	25-Sep-2009		120.5	13.973	3.890	118.403	5.505	5.482	5.513
12	26-Sep-2009		120.5	13.826	3.177	117.858	5.514	5.491	5.522
13	27-Sep-2009		120.5	13.706	2.403	117.285	5.524	5.502	5.533
14	28-Sep-2009		120.5	13.616	1.559	116.684	5.534	5.513	5.545
15	29-Sep-2009		120.5	13.558	0.635	116.054	5.546	5.526	5.557
16	30-Sep-2009	22-Jul-2010	122.0	13.085	2.057	115.769	5.510	5.489	5.521
17	01-Oct-2009		122.0	13.046	1.139	115.103	5.521	5.501	5.533
18	02-Oct-2009		122.0	13.042	0.125	114.408	5.535	5.514	5.547
19	03-Oct-2009	26-Jul-2010	123.9	12.454	2.587	114.251	5.483	5.461	5.494
20	04-Oct-2009		123.9	12.448	1.647	113.531	5.494	5.473	5.507
21	05-Oct-2009		123.9	12.476	0.599	112.781	5.507	5.487	5.521
22	06-Oct-2009		123.9	12.543	-0.575	111.997	5.521	5.502	5.536
23	07-Oct-2009		123.9	12.658	-1.902	111.174	5.539	5.520	5.555
24	08-Oct-2009		123.9	12.833	-3.410	110.293	5.559	5.541	5.576
25	09-Oct-2009	29-Jul-2010	125.4	12.300	-1.217	109.920	5.514	5.496	5.531
26	10-Oct-2009		125.4	12.478	-2.673	108.892	5.534	5.516	5.552
27	11-Oct-2009	01-Aug-2010	126.8	11.976	-0.188	108.475	5.492	5.473	5.509
28	12-Oct-2009		126.8	12.190	-1.574	107.540	5.511	5.493	5.530
29	13-Oct-2009		126.8	12.491	-3.210	106.570	5.534	5.518	5.555
30	14-Oct-2009		126.8	12.905	-5.127	105.556	5.564	5.548	5.585

= Maximum
= Minimum

*EME2000 coordinates at TIP for optimal launch time – i.e., middle of launch window.

Table 2: Baseline Launch Period Characteristics.

				Launch Vehicle Injection Targets*			Atmosphere-Relative Entry Speed (km/s)		
Launch Day	Lauch Date	Arrival Date	Ls (deg)	C_3 (km^2/sec^2)	DLA (deg)	RLA (deg)	Mawrth (24.88 N)	Meridiani (1.48 N)	Holden (26.37 S)
1	15-Oct-2009	4-Aug-10	127.8	12.339	-2.194	105.268	5.517	5.500	5.546
2	16-Oct-2009	5-Aug-10	128.3	12.432	-2.370	104.486	5.519	5.501	5.548
3	17-Oct-2009	6-Aug-10	128.8	12.554	-2.555	103.707	5.521	5.504	5.551
4	18-Oct-2009	8-Aug-10	129.7	12.706	-2.755	102.937	5.523	5.507	5.554
5	19-Oct-2009	9-Aug-10	130.2	12.891	-2.974	102.182	5.527	5.511	5.558
6	20-Oct-2009	11-Aug-10	131.2	12.695	-1.154	101.714	5.501	5.484	5.531
7	21-Oct-2009	12-Aug-10	131.7	12.908	-1.299	101.009	5.504	5.488	5.535
8	22-Oct-2009	13-Aug-10	132.1	13.151	-1.470	100.329	5.509	5.493	5.541
9	23-Oct-2009	15-Aug-10	133.1	12.986	0.598	99.957	5.482	5.466	5.512
10	24-Oct-2009			13.732	-1.923	99.050	5.522	5.506	5.555
11	25-Oct-2009	16-Aug-10	133.6	14.074	-2.226	98.452	5.530	5.515	5.564
12	26-Oct-2009	17-Aug-10	134.1	14.458	-2.601	97.882	5.541	5.526	5.576
13	27-Oct-2009	19-Aug-10	135.1	14.201	0.028	97.677	5.505	5.490	5.538
14	28-Oct-2009	20-Aug-10	135.6	14.582	-0.244	97.179	5.515	5.500	5.548
15	29-Oct-2009	23-Aug-10	137.0	13.888	5.368	97.352	5.445	5.427	5.472
16	30-Oct-2009	24-Aug-10	137.5	14.204	5.484	96.945	5.449	5.431	5.476
17	31-Oct-2009			15.122	2.288	96.231	5.496	5.481	5.528
18	01-Nov-2009	25-Aug-10	138.0	15.554	2.001	95.860	5.507	5.492	5.540
19	02-Nov-2009	26-Aug-10	138.5	16.028	1.585	95.508	5.521	5.506	5.554
20	03-Nov-2009	28-Aug-10	139.5	15.634	5.716	95.607	5.471	5.454	5.499
21	04-Nov-2009	30-Aug-10	140.5	15.411	9.785	95.715	5.429	5.410	5.452
22	05-Nov-2009	31-Aug-10	141.0	15.721	10.231	95.333	5.431	5.411	5.452
23	06-Nov-2009	1-Sep-10	141.5	16.039	10.964	94.952	5.432	5.412	5.453
24	07-Nov-2009	2-Sep-10	142.0	16.382	11.849	94.789	5.432	5.412	5.451
25	08-Nov-2009	3-Sep-10	142.5	16.714	12.997	94.669	5.429	5.408	5.447
26	09-Nov-2009	4-Sep-10	143.0	17.016	14.738	94.583	5.420	5.398	5.435
27	10-Nov-2009	5-Sep-10	143.5	17.271	17.867	94.566	5.402	5.378	5.411

= Maximum
= Minimum

*EME2000 coordinates at TIP for optimal launch time – i.e., middle of launch window.

Table 3: Extended Launch Period Characteristics.

Baseline Launch Period

Table 4 shows characteristics of MRO, ODY, and DTE EDL coverage for the baseline launch period. The minimum and maximum values are with respect to variations across the launch period. Data are provided for the Mawrth (North), Meridiani (Equatorial), and Holden (South) landing sites to illustrate how EDL coverage characteristics vary for with landing latitude. For MRO and ODY EDL coverage, the tables include mean anomaly range for orbiter phasing (see explanation in next section), antenna angle at entry, elevation at landing + 1 min, and required orbit node. The antenna angle and elevation data correspond to the middle of the mean anomaly range. For DTE EDL coverage, the following data are included: EDL visibility from separation to entry, antenna angle at entry, elevation at landing + 1 min, and percentage of total EDL duration that is visible. Values in red indicate where full DTE coverage is not possible.

Referring to Table 4, full EDL coverage is possible from MRO for all of the baseline launch period with the orbit node at the nominal value of 3:00 PM, except for northerly landing latitudes for several days at the end of the launch period. For days 27 through 30, the orbit node must be at 2:30 PM in order to provide full EDL coverage. The minimum mean anomaly range is 6 deg in the north and generally increases with deceasing latitude. The maximum MRO antenna angle at entry is close to 120 deg in the north and generally decreases with decreasing latitude. The minimum MRO elevation at landing + 1 min is always well above 10 deg. In general, MRO EDL coverage characteristics improve with decreasing latitude.

The EDL coverage situation is similar for ODY. The differences are that the orbit node must be at 2:30 PM for all landing latitudes for one or more days at the end of the launch period, and there is no definitive trend in antenna angle as a function of landing site latitude. Analyses have demonstrated that whenever MSL is in view from ODY, Earth is also in view, so that ODY can provide a real-time telemetry relay during EDL. MRO cannot provide this capability.

Figure 7 illustrates EDL coverage geometry for MRO and ODY for a trajectory targeted to Mawrth for launch at the open of the baseline launch period (15 September 2009). The plot shows the incoming MSL trajectory, the orbits of MRO and ODY, the landing site location, the directions to Earth and Sun and the directions from MSL to MRO and ODY. The labeled positions of MSL, MRO, and ODY correspond to the time of atmospheric entry, and the orbit nodes for MRO and ODY are at 3:00 PM. MRO is moving from south to north, and ODY is moving from north to south. The end points for the orbits of MRO and ODY are at the time of landing.

DTE EDL coverage for the baseline launch period (see Table 4) is always available from cruise stage separation to atmospheric entry (a hard requirement). However, because the launch/arrival strategy was not designed to provide full DTE EDL for all launch days and all latitudes, full DTE EDL coverage is in general possible only for launch dates toward the end of the launch period and only for northerly landing latitudes. Otherwise, EDL coverage ends some time after entry when MSL is occulted by Mars as viewed from Earth. EDL coverage extends to landing, or nearly to landing, for northerly and equatorial landing sites, but only to approximately one minute past entry for southerly landing sites. The maximum Earth antenna angle at entry is always well below 75 deg and increases with decreasing latitude. The minimum Earth elevation at landing + 1 min is below 10 deg for all landing latitudes gets progressively worse at equatorial and southerly landing site latitudes. In general, DTE EDL coverage characteristics degrade with decreasing latitude, a behavior that is opposite to that for MRO and ODY EDL coverage).

Extended Launch Period

Table 5 shows characteristics of MRO, ODY, and DTE EDL coverage for the extended launch period. For MRO and ODY EDL coverage for the extended launch

	Min/Max MA Range (deg)			Min/Max Ant Angle at Entry (deg)			Min/Max Elev at Lnd + 1^{m} (deg)			Required LMST Node (PM)*		
	North	Equatorial	South	North	Equatorial	South	North	Equatorial	South	North	Equatorial	South
MRO	6 21	10 19	19 22	109 118	106 115	88 101	21 60	28 79	18 33	3:00 (1) 2:30 (27)	3:00	3:00
ODY	6 32	8 30	14 28	101 117	108 119	106 120	22 60	26 51	15 35	3:00 (1) 2:30 (30)	3:00 (1) 2:30 (25)	3:00 (1) 2:30 (27)

	Visibility from SEP to Entry?			Min/Max Ant Angle at Entry (deg)			Min/Max Elev at Lnd + 1^{m} (deg)			Min/Max EDL Coverage (%)**		
	North	Equatorial	South	North	Equatorial	South	North	Equatorial	South	North	Equatorial	South
DTE	Y	Y	Y	14 27	26 38	40 53	7 20	-2 9	-17 -11	83% 100%	79% 88%	13% 21%

North = Mawrth (24.65 N) Equatorial = Meridiani (1.48 N) South = Holden (26.37 S)
*Number in parentheses is first launch day at which node value applies.
**Coverage starts at entry and ends when Mars occults MSL as seen from Earth.

Table 4: Baseline Launch Period EDL Coverage Characteristics: Variations Across 30 Launch Days.

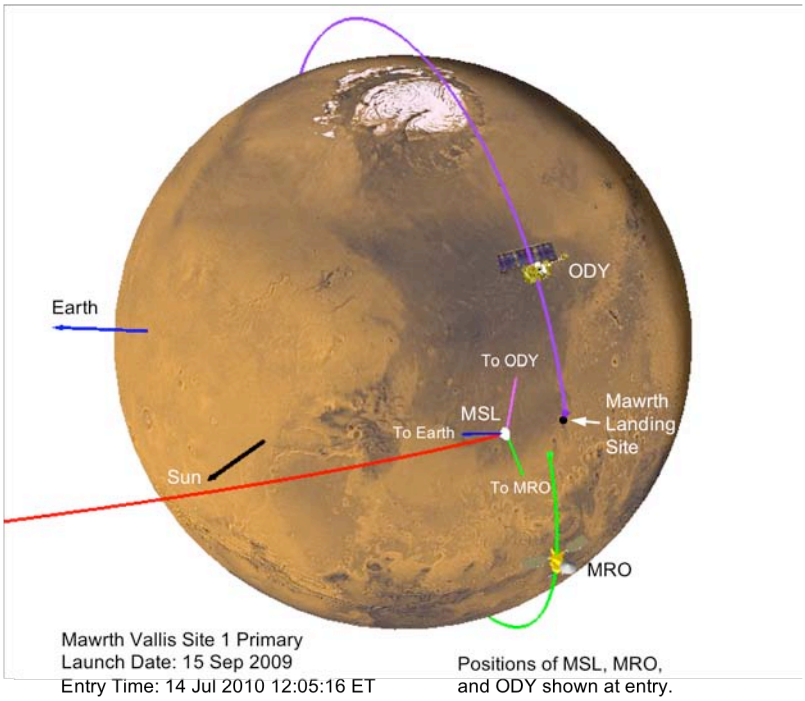

Figure 7: EDL Coverage Geometry – Mawrth (15 September 2009 Launch).

period (see Table 5), the most significant difference from the baseline launch period is that the LMST of the orbit node must be moved progressively earlier as the launch period progresses in order to be able to provide full EDL coverage. For developing the launch/arrival strategy, the LMST is moved earlier in steps of 30 min. For equatorial and southerly latitudes, the steps occur later – i.e., any given LMST can be maintained for a greater number of launch days.

As compared to the baseline launch period, mean anomaly ranges, antenna angles at entry, and elevations at landing + 1 min are very similar, with the exception that the minimum mean anomaly ranges are somewhat lower. As for the baseline launch period, ODY can provide a real-time telemetry relay during EDL.

DTE EDL coverage for the extended launch period (see Table 5) is significantly improved as compared to the baseline launch period, because Earth visibility of EDL is more favorable at later arrival days. The Earth elevations at landing + 1 min are significantly higher. Full, or nearly full, DTE coverage is possible for the entire extended launch period for northerly and

	Min/Max MA Range (deg)			Min/Max Ant Angle at Entry (deg)			Min/Max Elev at Lnd + 1^{m} (deg)			Required LMST Node (PM)*		
	North	Equatorial	South	North	Equatorial	South	North	Equatorial	South	North	Equatorial	South
MRO	5 22	7 19	14 21	110 119	104 117	72 101	26 74	37 86	13 51	2:30 (1) 2:00 (6) 1:30 (14) 1:00 (20) 12:30 (25)	2:30 (1) 2:00 (9) 1:30 (15) 1:00 (21) 12:30 (27)	2:30 (1) 2:00 (9) 1:30 (15) 1:00 (21) 12:30 (27)
ODY	9 25	5 32	5 27	101 117	111 119	103 118	30 48	21 46	11 31	2:30 (1) 2:00 (4) 1:30 (10) 1:00 (17) 12:30 (24)	2:30 (1) 2:00 (3) 1:30 (10) 1:00 (17) 12:30 (24)	2:30 (1) 2:00 (5) 1:30 (13) 1:00 (20) 12:30 (24)

	Visibility from SEP to Entry?			Min/Max Ant Angle at Entry (deg)			Min/Max Elev at Lnd + 1^{m} (deg)			Min/Max EDL Coverage (%)**		
	North	Equatorial	South	North	Equatorial	South	North	Equatorial	South	North	Equatorial	South
DTE	Y	Y	Y	26 45	37 48	53 62	22 48	11 13	-10 22	100% 100%	91% 100%	22% 91%

North = Mawrth (24.65 N) Equatorial = Meridiani (1.48 N) South = Holden (26.37 S)
*Number in parentheses is first launch day at which node value applies.
**Coverage starts at entry and ends when Mars occults MSL as seen from Earth.

Table 5: Extended Launch Period EDL Coverage Characteristics: Variations Across 27 Launch Days.

equatorial landing latitudes. For southerly latitudes, only partial EDL coverage is possible, ranging from slightly more than one minute to nearly complete coverage. Values in red indicate where full DTE coverage is not possible

Launch Trajectory Characteristics

The key factors for MSL launch trajectory design are time of launch, time from launch to eclipse exit, and DSN initial acquisition characteristics.

Due to additional range safety requirements for a launch payload containing radioisotope materials, MSL launch must occur during daylight. Daylight is defined to be no earlier than the beginning of morning civil twilight and no later than the end of evening civil twilight. The beginning of morning civil twilight and the end of evening civil twilight are defined to occur when the center of the Sun is geometrically 6 deg below the horizon. Figures 8 and 9 show plots of launch time as a function of launch date for open, middle, and close of a 2 hr launch window (maximum duration) for the baseline and extended launch periods. The plots also show daylight time constraints as appropriate. All launch times occur during daylight.

Approximately 7 min prior to launch, the MSL spacecraft transfers to internal power. After separation from the Centaur upper stage and exit from eclipse, the spacecraft solar arrays will provide electrical power to

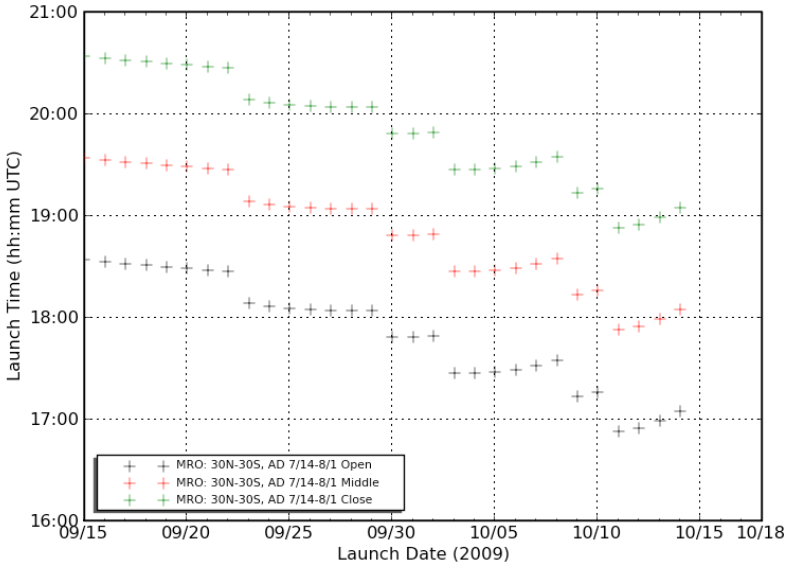

Figure 8: Launch Times – Baseline Launch Period.

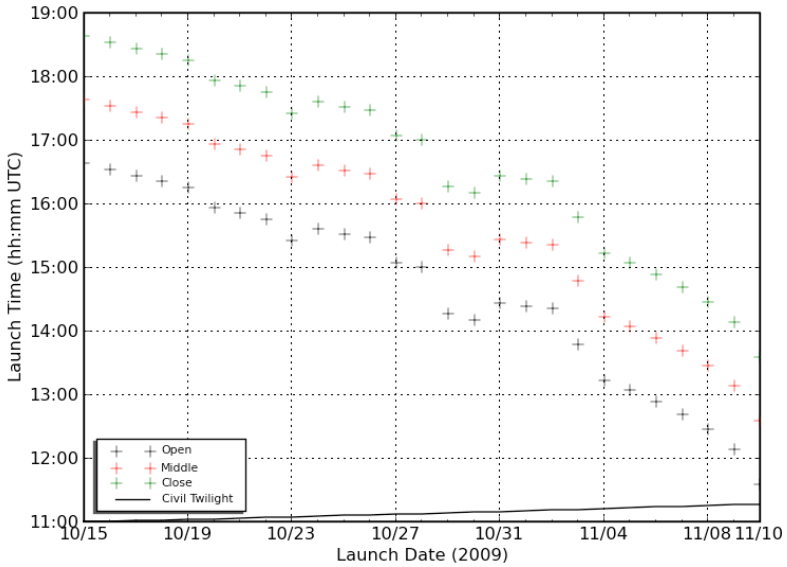

Figure 9: Launch Times – Extended Launch Period.

the spacecraft systems. In order not to exceed the spacecraft battery capacity, the time from launch to eclipse exit or spacecraft separation, whichever is later, must be less than 65 min. Because eclipse exit always occurs after separation, this requirement defaults to the eclipse exit time. Figures 10 and 11 show plots of time from launch to eclipse exit as a function of launch date for open, middle, close of a 2 hr launch window (maximum duration) for the baseline and extended launch periods. The plots also show the 65 min constraint. Missing data points for open, middle, or close of the launch window indicate that no eclipse occurs for that launch date and time. For the baseline launch period, there is considerable margin against the constraint. For the extended launch period, the time from launch to eclipse exit increases, and on days 26 and 27, the constraint is violated either for part or all of the launch window. As this paper was being prepared, the MSL project has decided to implement a strategy that allows the spacecraft solar arrays to charge the battery whenever they are illuminated between parking orbit insertion and eclipse entry in order to provide adequate power margin for the end of the extended launch period

Initial acquisition of the spacecraft radio signal by the DSN can occur after activation of the spacecraft radio transmitter (following separation from the Centaur and eclipse exit) and after a DSN complex has

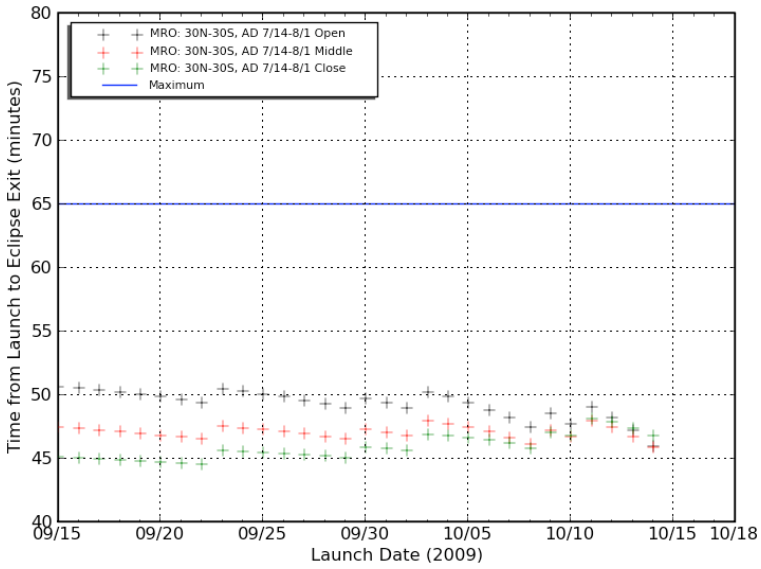

Figure 10: Time from Launch to Eclipse Exit – Baseline Launch Period.

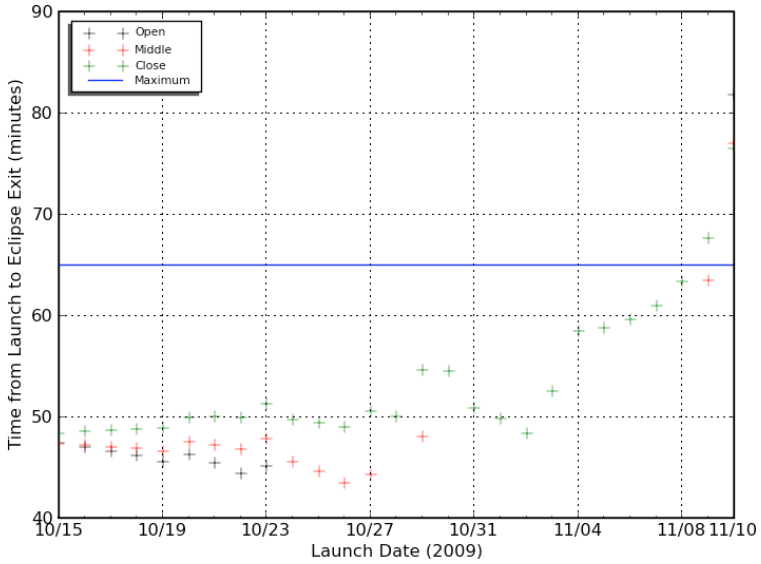

Figure 11: Time from Launch to Eclipse Exit – Extended Launch Period.

the spacecraft in view. As noted earlier, eclipse exit always occurs after spacecraft separation, so that transmitter turn-on occurs no earlier than eclipse exit. Canberra is always the first DSN complex to have the spacecraft in view, and this usually occurs after eclipse exit; however, for launches near the close of the launch window for launch days toward the end of the extended launch period, eclipse exit is after Canberra rise. A ground track plot for launch on 15 September 2009 at open of the launch window is shown in Figure 12.

- Minimize operational complexity.
- Minimize atmospheric entry delivery errors.
- Minimize total cruise propellant usage.

TCMs 4, 5, and 6 occur during the approach phase, which starts at E – 45 days. These TCMs adjust the trajectory to the desired atmospheric entry conditions. TCM-5 at E – 2 days is the final entry targeting maneuver for landing site safety – i.e., TCM-5 is the last maneuver required to achieve the EFPA delivery accuracy requirements. TCM-6 at E – 7 hrs is the final

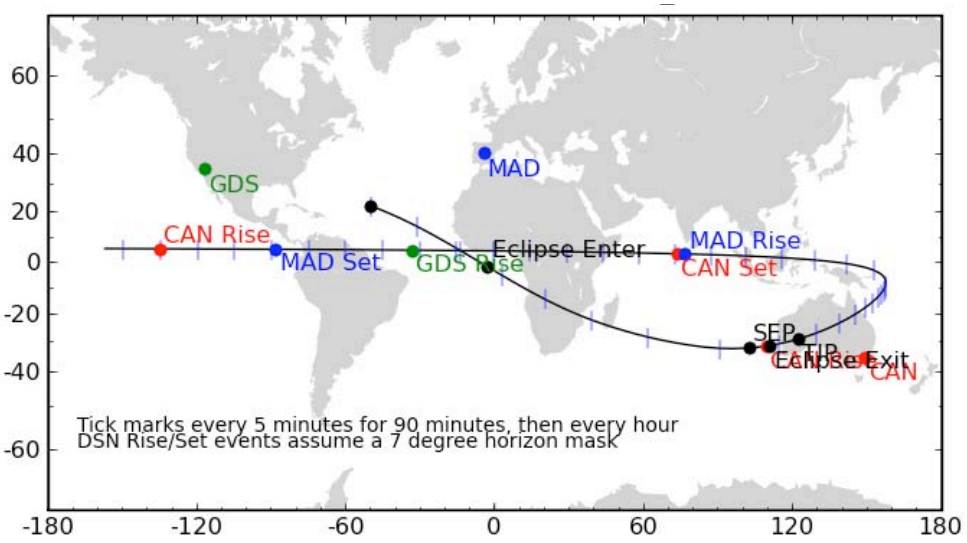

Figure 12: Ground Track Plot for Launch on 15 September 2009 at Open of Launch Window (GDS = Goldstone, MAD = Madrid, CAN= Canberra).

NAVIGATION DESIGN

This section addresses the TCM profile, orbit determination analysis, and propulsive maneuver analysis. Orbit determination analysis includes atmospheric entry delivery and knowledge accuracies and approach navigation sensitivities. Propulsive maneuver analysis includes injection aimpoint biasing, non-nominal impact probability, TCM ΔV and propellant statistics, and landing site retargeting.

TCM Profile

In order to achieve the atmospheric entry delivery accuracy requirement for EFPA, five nominal and two contingency TCMs are planned during the cruise and approach phases. Table 1 lists the name, nominal execution time, and a description of the maneuver for each TCM. The TCM locations are chosen as a compromise between competing requirements:

- Provide sufficient time between launch and TCM-1 for spacecraft checkout and design of TCM-1.
- Provide sufficient time between TCMs to allow for TCM reconstruction, orbit determination, and sequence generation for the upcoming TCM.

opportunity to adjust the trajectory. In the event that there has been an anomaly during or after TCM-5 (or TCM-5X) that causes an unwanted ΔV, or for any other reason a late TCM is required, TCM-6 is the final opportunity to ensure that the delivery accuracy requirements are met. Although TCM-6 is a contingency maneuver, it is being prepared for in exactly the same manner as the other approach phase maneuvers.

The navigation tracking data cutoff time for TCMs 1 through 3 is 5 days prior to the TCM; for TCMs 4, 5, and 5X, the data cutoff is 12 hours prior to the TCM; for TCM-6, the data cutoff is 5 hours prior to the TCM. The data cutoffs for the final four TCMs are closer to execution of the TCM in order to reduce navigation tracking data latency, thereby improving entry delivery accuracy. All TCMs utilize the so-called "Auto-TCM" behavior, similar to that developed for MER. The commands to execute the TCM are part of flight software. The ground TCM design process determines a set of parameters that govern the execution of the TCM, and these parameters are uplinked to the spacecraft prior to scheduled execution. The "Auto-TCM" behavior also includes logic that can detect faults and,

after recovery from the fault, resume execution of the TCM.

Orbit Determination (OD)

Radiometric Data Accuracy

The baseline radiometric data types used for orbit determination are two-way coherent Doppler, two-way ranging, and Delta Differential One-way Range (ΔDOR) measurements generated by the DSN X-band tracking system. All data types are derived from a coherent radio link between the spacecraft and a receiver at a DSN ground station. In the case of ΔDOR measurement, a radio signal from a quasar will also be used to obtain the measurements.

Doppler data yield a measurement of line-of-sight spacecraft range rate. During tracking passes in the two-way coherent mode of operation, the DSN tracking system measures Doppler shift by accumulating the cycles of the downlink carrier signal in order to determine the difference between the transmitted and received frequencies.

Two-way range is also a line-of-sight measurement. The DSN ranging system constructs an estimate of the range to the spacecraft by measuring the round-trip light time of a radio signal between the ground station and the spacecraft.

ΔDOR is a Very Long Baseline Interferometry measurement of a spacecraft using pairs of DSN stations (either Goldstone-Madrid or Goldstone-Canberra) and an intergalactic radio source (i.e., quasar). Two DSN stations simultaneously observe the spacecraft followed by simultaneous observations of the quasar. ΔDOR directly measures angular separation between the spacecraft and the quasar in the direction of the projected baseline between the two stations. The ΔDOR observable is a phase delay time expressed in units of nanoseconds (ns) that is equivalent to an angular separation between the spacecraft and the quasar; a delay of 1 ns corresponds to an angular separation of ~37.5 nrad. ΔDOR measurements determine the spacecraft position in the plane of the sky. The Goldstone-Madrid baseline (oriented East-West) primarily measures the right ascension component of the spacecraft position, and the Goldstone-Canberra baseline (oriented Northeast-Southwest) primarily measures the declination component of the spacecraft position, with a substantial dependency on right ascension as well. ΔDOR measurements are generally scheduled with alternating baselines. The ΔDOR data type complements line-of-sight Doppler and range measurements because of its orthogonality to those data types. Furthermore, ΔDOR and range data provide a near-instantaneous measurement of spacecraft position and thus do not rely on dynamic models to infer position, as is the case with Doppler and range.

The assumed radiometric data accuracies for MSL orbit determination analyses are as follows (Ref. 3):

Doppler	0.1 mm/s (1σ)
Range	3.0 m (1σ)
ΔDOR	2.4 nrad (1σ)

In addition, quasar location errors are assumed to be 1.0 nrad (1σ).

Navigation Tracking Schedule

The DSN 34-meter High Efficiency (HEF) subnet will be utilized for acquisition of Doppler, range, and ΔDOR data for navigation. The tracking schedule used for orbit determination analyses is shown in Table 6.

Doppler and range tracking coverage is continuous for the first 30 days following launch and for the entire approach phase starting at E – 45 days. ΔDOR measurements start approximately 30 days after launch,

Time Span	Doppler/Range	ΔDOR
Launch to L + 30 days	Continuous	None
L + 30 days to E – 45 days	3 8-hr passes per week	1 point per week
E – 45 days to E – 28 days	Continuous	2 points per week
E – 28 days to Entry	Continuous	2 points per day

Table 6: DSN Tracking Schedule.

and the frequency increases to two points per day (with alternating baselines) during the final 28 days prior to entry. The final two ΔDOR measurements prior to the navigation data cutoff for a TCM design are not included for analysis purposes to account for ΔDOR data processing latency.

OD Filter Assumptions

The orbit determination analysis results presented below are based on linear covariance analyses that simulate orbit determination processing with a multiple batch consider-parameter filter. The baseline OD filter assumptions are shown in Table 7 and discussed below.

Radiometric data accuracies and the navigation tracking schedule were discussed previously. For each tracking pass, constant Doppler and range data biases are estimated.

All TCMs contained within the data arc are also estimated. Future TCMs occurring after the navigation data cutoff time are treated in one of two ways. For generating entry delivery uncertainties, the TCM directly after the data cutoff time is "considered" in the filter at the a priori uncertainty, while any other future TCMs are ignored. For a consider parameter, the error source is included at the a priori value, but the parameter is not estimated. For generating orbit

determination covariances for propulsive maneuver analyses, all future TCMs are ignored, and maneuver execution errors are modeled in the maneuver analysis process.

ACS ΔV events (i.e., residual ΔV caused by spacecraft turns for attitude maintenance) that fall within the data arc are estimated, and future events are considered. Each ΔV from an ACS event is modeled with a three-component impulse.

The solar pressure model consists of a single flat plate representing the solar array and the area inside of the solar array, including the launch vehicle adaptor. In addition, a cylinder model represents the launch vehicle adaptor and the heat rejection system, while an antenna model represents the backshell. The antenna model accounts for shadowing of the backshell from the cruise stage as a function of solar aspect angle. Each component has a mean specular and diffuse coefficient of reflectivity associated with it, and a reflectivity degradation schedule. Use of this high-fidelity solar pressure model eliminates the need to include an error source for unmodeled non-gravitational accelerations in the OD filter.

Other stochastically estimated parameters include Earth orientation parameters (pole X/Y and UT1[§]), media effects (troposphere and ionosphere), and Earth and Mars ephemerides. The considered parameters are

Error Source	Estimated/ Considered	A Priori Uncertainty (1σ)	Correlation Time	Update Time	Comments
X-Band 2-way Doppler (mm/s)	–	0.1	–	–	
Range (m)	–	3	–	–	
ΔDOR (ns)	–	0.06	–	–	Equivalent to 2.4 nrad.
Epoch State Position (km)	Est.	1000	–	–	
Epoch State Velocity (km/s)	Est.	1	–	–	
Solar Radiation Pressure					Three-component high-fidelity model. Correlation broken at turns. Gr, Gx estimated both as bias and stochastic.
Gr = Radial Component (%)	Est.	5	7 days	1 day	
Gx = Tangential Component (%)	Est.	5	7 days	1 day	
Gy = Out-of-Plane Component (%)	Est.	1	–	–	
Doppler Bias (mm/s)	Est.	0.002	0	Per pass	
Range Bias (m)	Est.	2	0	Per pass	
Mars & Earth Ephemerides	Est.	DE414 Covariance	–	–	Based on analysis assuming one ΔDOR per month from MRO/ODY for one Earth/Mars synodic period prior to MSL arrival.
Mars GM (km^3/s^2)	Est.	2.8×10^{-4}	–	–	From PHX.
Station Locations (cm)	Con.	Full 2003 Covariance	–	–	
Quasar Locations (nrad)	Con.	1	–	–	
Earth Orientation Parameters					
Pole X/Y (cm)	Est	1 → 4	48 hrs	6 hrs	Ramp from 2 days before EOP delivery to EOP + 12 hr.
UT1 (cm)	Est	1.7 → 15	48 hrs	6 hrs	Ramp from 6 days before EOP delivery to EOP + 12 hr.
Ionosphere – Day/Night (cm)	Est	55/15	6 hrs	1 hr	S-band units. Use 6x (ionosphere) and 2x (troposphere) apsig when no actuals. Subsequent passes are uncorrelated.
Troposphere – Wet/Dry (cm)	Est	1/1	6 hrs	1 hr	
ACS Event ΔV – Per Axis (mm/s)	Est.	2 mm/s before E – 45 days, 1 mm/s after E – 45 days	–	–	Turns occur at L + 15 days and every 7 days thereafter up to E – 8 days. Uncertainties are per flight system requirements.
Non-gravitational Accelerations (km/s^2)	–	0	–	–	Removed because of improved solar radiation pressure model.
TCM Execution Errors (mm/s)	Est.	Magnitudes of TCM execution errors are specific to each trajectory.			
TCM-1 (L + 15 days)					8% proportional error (3σ); 4 mm/s fixed error (3σ), turn/burn maneuver.
TCM-2 (L + 120 days)					8% proportional error (3σ); 4 mm/s fixed error (3σ); vector mode maneuver.
TCM-3 (E – 60 days)					
TCM-4 (E – 8 days)					
TCM-5 (E – 2 days)					

Table 7: Baseline Orbit Determination Filter Assumptions.

[§] UT1 is the principal form of Universal Time that is corrected for the effect of polar motion and is proportional to the true rotation angle of the Earth with respect to a fixed frame of reference.

quasar locations and DSN station locations, since tracking data does not improve estimates of these quantities.

In addition to the baseline OD filter assumptions, a set of "No Margin" assumptions is also used. The "No Margin" scenario applies the following assumptions:

- Unlikely faults and out-of-spec performance (both accounted for in the baseline assumptions) do not occur.
- All requested Doppler and range tracking passes are successful.
- All requested ΔDOR measurements are successful, and the data processing latency is consistent with performance for past missions.

The difference in navigation performance between the "No Margin" and baseline assumptions quantifies the level of margin included in the navigation design. The "No Margin" OD filter assumptions have the following changes with respect to the baseline assumptions listed in Table 7 (all values 1σ unless otherwise noted):

- Doppler accuracy = 0.05 mm/s.
- ΔDOR accuracy = 0.04 ns (1.6 nrad).
- Gr (radial) and Gx (tangential) errors for solar radiation pressure = 2%.
- Range bias = 1 m.
- Pole X/Y errors = 1 cm (constant value).
- Upper limit on UT1 error = 7.5 cm.
- Fixed maneuver execution error = 2 mm/s (3σ).

Approach Navigation Accuracies

The combination of orbit determination errors and maneuver execution errors mapped to the atmospheric entry interface point is referred to as TCM delivery accuracy. Atmospheric entry knowledge accuracy for position or velocity is the OD knowledge accuracy at entry (computed from the position or velocity covariance norm) based on an OD data cutoff at E – 6 hrs. This section presents results for entry delivery and knowledge accuracies based on linear covariance analyses that use the models and assumptions discussed above. TCMs 4 and 5 during the approach phase are the key maneuvers for targeting to the desired entry interface conditions. The entry interface targets are EFPA, B-plane angle, and entry time (see Figure 13).

Targeting a specific B-plane angle and entry time corresponds to targeting a specific latitude and longitude on the surface. Given a desired landing site target and EFPA value, the values for B-plane angle and entry time are determined from an EDL trajectory simulation that varies the entry conditions to achieve the desired landing site latitude and longitude. The EFPA is selected based on results of EDL Monte Carlo simulations to evaluate the performance of the entry guidance algorithm. For MSL, the nominal EFPA is -15.5 deg, although a shallower (i.e., less negative) value may be used.

EFPA error is proportional to the error in the magnitude of the B-vector that depends on the B-plane angle and the orientation of the B-plane error ellipse. Figure 14 illustrates the dependence of EFPA error on B-plane angle for a fixed error ellipse orientation. If the semi-major axis of the error ellipse lies along the B-vector (Ellipse 1), the EFPA error is maximized. If

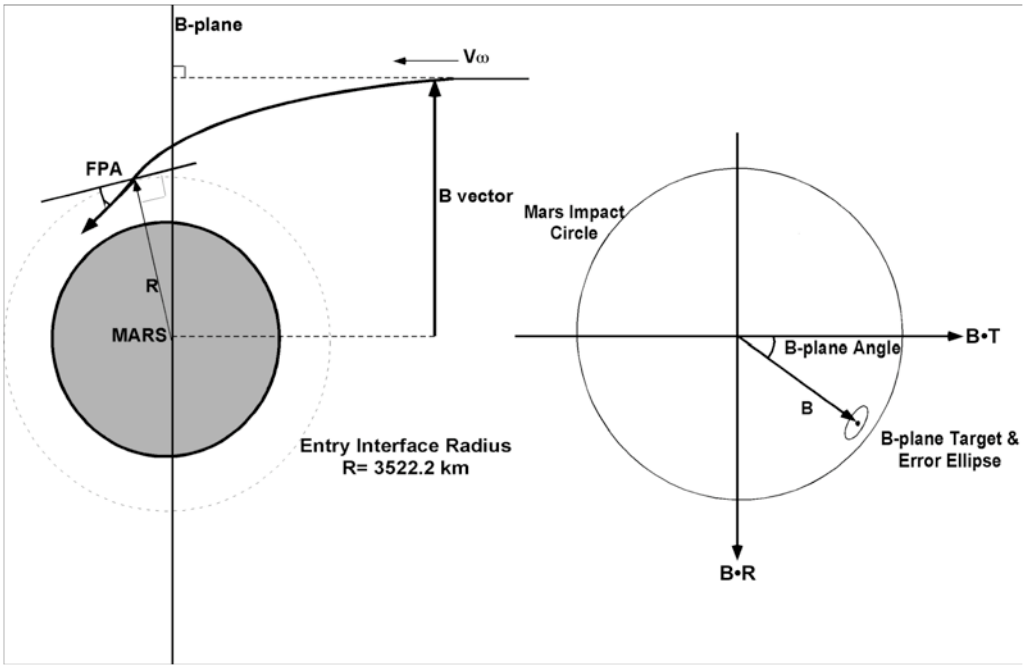

Figure 13: Entry Interface Point, B-plane, and B-plane Angle.

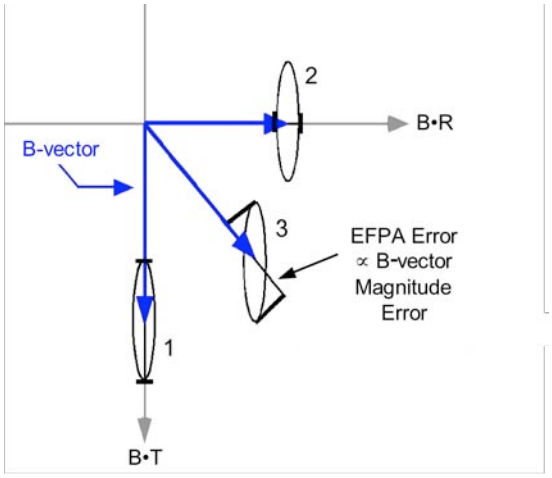

Figure 14: Dependence of EFPA Error on B-plane Angle.

the semi-minor axis of the error ellipse lies along the B-vector (Ellipse 2), the EFPA error is minimized. Ellipse 3 illustrates an intermediate case. In a similar fashion, assuming the B-plane angle is fixed, the B-vector magnitude error will vary as the orientation of the error ellipse changes. For the cases that have been analyzed for MSL, the size, shape, and orientation of the B-plane error ellipse does not vary for a given TCM, so that B-plane angle is a more important factor for determining EFPA error.

EFPA error is also a function of the targeted EFPA. Steeper (i.e., more negative) EFPA values produce smaller EFPA errors; likewise, shallower (i.e., less negative) EFPA values produce larger EFPA errors. At the nominal EFPA of –15.5 deg, a change in EFPA of +1.0 deg causes EFPA error to increase by less than 0.01 deg, which is a small effect.

The cases selected for analyzing entry delivery and knowledge curacies are shown in Table 8. The launch date / arrival date combinations correspond to open and close of the baseline and extended launch periods. For the baseline launch period cases, the landing latitudes correspond to the northern and southern limits of possible latitude range plus an equatorial case. For the extended launch period, it was decided to use actual candidate landing sites with extreme northerly and southerly latitudes.

Launch Period	Launch Date	Arrival Date	Landing Latitudes / Sites
Baseline	15-Sep-2009 14-Oct-2009	14-Jul-2009 1-Aug-2010	30N, 0, 30S
Extended	15-Oct-2009 10-Nov-2009	4-Aug-2010 5-Sep-2010	Nili (21.0N), Holden (26.4S)

Table 8: Approach Navigation Analysis Cases.

The entry delivery and knowledge accuracy results for the above cases are shown in Table 9. The TCM-4 and TCM-5 delivery errors assume a navigation data cutoff 12 hrs prior to the TCM. The entry knowledge errors assume a data cutoff at E – 6 hrs.

The values for the TCM-4 EFPA delivery error are very similar for the different cases, with the exception of the case at close of the extended launch period for the Nili landing site. The TCM-5 EFPA delivery errors exhibit the same behavior. The EFPA delivery requirement is met, or nearly met, at TCM-4 and always met at TCM-5 with ample margin. With "No Margin" assumptions, EFPA errors improve significantly, such that the delivery requirement is always met at TCM-4. These results indicate that it is unlikely that TCM-5 will be required.

For entry state knowledge, the requirements for position and velocity accuracy are always met with significant margin. Entry knowledge errors are smallest at northerly latitudes and increase as landing latitude moves south. As expected, "No Margin" assumptions significantly improve entry knowledge.

Figure 15 shows 3σ B-plane error ellipses for the case at open of the baseline launch period targeted to a

Launch Period	Launch Date	Arrival Date	Landing Latitude / Site	3σ EFPA Delivery Error (deg)				3σ Entry State Knowledge Error*			
				TCM-4		TCM-5		Position (km)		Velocity (m/s)	
				Baseline	No Margin	Baseline	No Margin	Baseline	No Margin	Baseline	No Margin
Baseline	15-Sep-2009	14-Jul-2010	30N	±0.22	±0.16	±0.09	±0.05	1.1	0.9	0.9	0.7
			0	±0.21	±0.16	±0.08	±0.05	1.7	1.3	1.2	0.9
			30S	±0.21	±0.16	±0.08	±0.05	1.9	1.4	1.3	1.0
	14-Oct-2009	1-Aug-2010	30N	±0.19	±0.11	±0.08	±0.04	1.3	1.0	1.0	0.7
			0	±0.20	±0.11	±0.08	±0.05	1.9	1.4	1.4	1.0
			30S	±0.21	±0.12	±0.08	±0.05	2.1	1.6	1.5	1.1
Extended	15-Oct-2009	4-Aug-2010	Nili (21.0N)	±0.19	±0.12	±0.07	±0.04	1.4	1.0	1.0	0.8
			Holden (26.4S)	±0.21	±0.14	±0.08	±0.05	2.0	1.6	1.4	1.1
	10-Nov-2009	5-Sep-2010	Nili (21.0N)	±0.15	±0.10	±0.04	±0.02	1.1	0.9	0.9	0.7
			Holden (26.4S)	±0.19	±0.13	±0.07	±0.05	2.1	1.7	1.6	1.2
Requirement				±0.20				2.8		2.0	
*Arbitrarily defined as three times the position or velocity covariance norm.											

Table 9: Entry Delivery and Knowledge Accuracy Results.

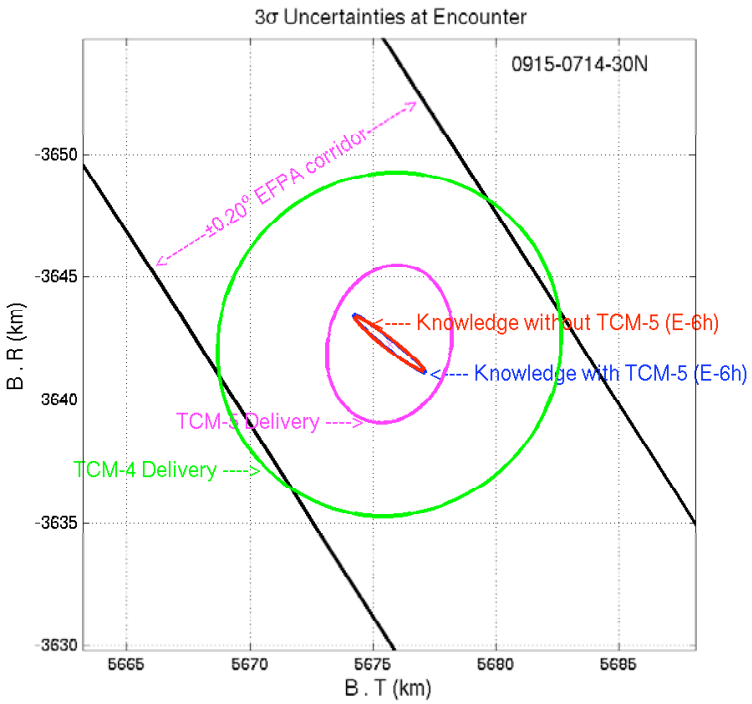

Figure 15: B-plane Error Ellipses: Launch on 15 September 2009, 30N Latitude.

30N landing latitude. Ellipses are included for TCM-4 and TCM-5 delivery uncertainties and for entry knowledge uncertainty. The TCM-4 error ellipse slightly exceeds the ±0.20 deg EFPA delivery requirement. Note that the TCM-4 error ellipse is nearly circular, which is typical for all cases studied. This explains why TCM-4 EFPA errors are insensitive to landing latitude (see Table 9) for all but one case. The TCM-5 error ellipse is more eccentric, but the effect is not large, and TCM-5 EFPA errors are also insensitive to landing latitude. There are two entry knowledge ellipses that are virtually identical. One assumes TCM-4 is the final maneuver (a likely scenario); the other assumes TCM-5 is the final maneuver. Whether or not TCM-5 is performed has little effect on entry knowledge accuracy. The entry knowledge ellipses show that between TCM-5 and the E – 6 hr navigation data cutoff for entry knowledge, the uncertainties have been reduced mostly in the EFPA direction (i.e., along the B-vector).

Approach Navigation Sensitivities

In order to understand the effects on entry delivery and knowledge accuracies of changes in OD filter assumptions and navigation data assumptions, a series of sensitivity studies have been performed. Navigation data assumptions include data types, data quantity, and, for entry knowledge errors, the navigation data cutoff time. The "No Margin" results discussed in the previous section represent one type of sensitivity study where multiple assumptions have been changed. For each of the sensitivity studies discussed in this section, only one parameter is changed with respect to the baseline assumptions to understand the effect of only that parameter. Each of the error sources for the OD filter (see Table 7) is changed to an "improved" value and a "degraded" value. In general, the baseline value is halved and doubled to produce the improved and degraded values.

Due to space limitations, the quantitative results for all the sensitivity studies cannot be included here. The sensitivity results are summarized in Table 10 and discussed below.

TCM-4 EFPA delivery accuracy is most sensitive to TCM-4 execution errors and ACS event ΔV. Doubling any one of these error sources causes the ±0.20 deg (3σ) EFPA delivery requirement (marginally met at TCM-4) to be violated. For TCM-5, the EFPA delivery accuracy is most sensitive to TCM 4 and 5 execution errors and ΔDOR accuracy and latency. However, the EFPA delivery requirement can still be met even if any of these error sources is doubled. Entry knowledge accuracy is most sensitive to Earth-Mars ephemeris errors, ΔDOR accuracy and latency, and quasar location errors. Doubling any of these error sources does not cause the entry knowledge requirement to be violated.

In general, if all ΔDOR data or all range data are deleted, TCM 4 and 5 EFPA delivery accuracies and entry knowledge accuracies degrade to the point that

Sensitivity Type	Baseline Value	Change	Results
OD Filter Assumptions	Table 7	Halved or Doubled	Largest sensitivities for TCM-4 delivery: • TCM-4 execution error • ACS event ΔV Largest sensitivities for TCM-5 delivery: • TCM 4 & 5 execution errors • ΔDOR accuracy & latency Largest sensitivities for entry knowledge: • Earth-Mars ephemeris errors • ΔDOR accuracy & latency • Quasar location errors
Data Types / Quantity	Doppler, Range, & ΔDOR	Delete data type(s)	• TCM-4 delivery requirement violated if all ΔDOR and/or all range data removed. • TCM-5 delivery requirement violated if all ΔDOR data removed. • Entry knowledge requirement violated if all ΔDOR and/or all range data are removed.
Entry Knowledge Data Cutoff Time	E – 6 hrs	E – 33 hrs	Position uncertainties (with TCM-5): 2.5 - 4.0 km for baseline launch period 3.0 - 7.0 km for extended launch period No TCM-5 ⇒ ~20% improvement. "No Margin" ⇒ ~30% improvement. Velocity uncertainties (with TCM-5): 1.5 - 3.0 m/s for baseline launch period 3.0 - 7.0 m/s for extended launch period No TCM-5 ⇒ ~15% improvement. "No Margin" ⇒ ~30% improvement.

Table 10: Approach Navigation Sensitivity Study Results.

their respective requirements are violated. The requirements can still be achieved, however, if only a small amount of range data (a few hours per day during the approach phase) and partial ΔDOR data (only East-West or only Northeast-Southwest baselines) are available.

The navigation data cutoff for the final estimate of the entry state vector to be uplinked to the spacecraft for use by the onboard entry guidance algorithm is nominally at E – 6 hrs. It would be desirable to move the data cutoff earlier to allow more processing time for orbit determination and to uplink a sufficiently accurate estimate of the entry state significantly earlier relative to atmospheric entry. The next earlier opportunity to uplink the entry state to the spacecraft corresponds to a data cutoff time at E – 33 hrs. Unfortunately, with this data cutoff time, the entry knowledge requirements (2.8 km and 2.0 m/s, both 3σ) are generally violated, except for certain cases for the baseline launch period. However, with the earlier data cutoff time, the entry knowledge accuracy can be improved significantly either by assuming TCM-5 is not executed (very likely) or by taking advantage of the "No Margin" results. Some combination of these two effects should enable the entry knowledge requirement to be met.

The sensitivity results demonstrate that, in general, entry delivery and knowledge accuracies are fairly robust to degradations to OD filter assumptions and navigation data assumptions.

Propulsive Maneuver Analysis

Maneuver Strategy

TCMs are required to compensate for launch vehicle injection errors, injection aimpoint biasing for planetary protection, orbit determination errors, and maneuver execution errors and to accommodate landing site retargeting after launch. Landing site retargeting is discussed in more detail in a subsequent section. TCMs are inherently statistical in nature (i.e., non-deterministic), since they are required to correct for trajectory dispersions from various error sources. However, TCMs may have a deterministic component. The maneuver strategy described in this section attempts to minimize total cruise statistical ΔV and propellant usage while satisfying all mission requirements and spacecraft constraints.

The goal of the maneuver strategy is to minimize the total required cruise propellant for TCMs and spacecraft attitude/spin control while satisfying various mission constraints, such as launch vehicle and spacecraft planetary protection requirements. The high-level maneuver strategy used for the results presented in this section assumes that for the design of the reference interplanetary trajectory TCMs 1 and 2 may have deterministic components in order to minimize the ΔV cost to remove Mars aimpoint biasing for planetary protection and to retarget the landing site. For statistical Monte Carlo maneuver analyses, the total ΔV for TCMs

1, 2, and 3 are optimized to minimize the total ΔV cost in the presence of dispersions and to satisfy the spacecraft non-nominal impact probability requirement.

Maneuver Analysis Assumptions

The assumptions used for propulsive maneuver analyses reported in this paper are as follows:

- The TCM profile is as given in Table 1.
- A spacecraft turn is permitted at TCM-1; all subsequent TCMs must be performed at the nominal cruise attitude[**].
- The total spacecraft mass at injection onto the interplanetary trajectory is 4100 kg.
- The spacecraft is spin-stabilized during cruise at a nominal spin rate of 2 rpm.
- The total cruise stage usable propellant load for TCMs and attitude/spin control during interplanetary cruise is 70 kg.
- The nominal thrust level of the cruise stage thrusters at initial propellant tank pressure is 4.7 N.
- The effective I_{sp} values for axial and lateral maneuvers are 212.4 s and 221.8 s, respectively. (These values reflect blowdown effects during cruise have been adjusted to account for thruster plume impingement losses of 6% for axial burns and 1% for lateral burns.)
- The lateral ΔV direction is at an angle of 100.6 deg from the spacecraft –Z axis. (This results from a propulsion system constraint that the lateral ΔV vector must be directed through the spacecraft center of mass in order not to cause spacecraft attitude perturbations during TCMs.)
- The spacecraft –Z axis off-Earth and off-Sun angles at TCM-1 must be less than 75 deg and 50 deg[§]. (These constraints ensure that there will be a communications link with Earth and adequate spacecraft power margin at TCM-1.)
- Thruster burn penalties caused by thruster cant angles (see Figure 16) are 55.6% for axial burns and 30.5% for lateral burns; the finite burn arc penalty for lateral burns (60 deg burn arc; 5 s burn) is 4.7%[§].

Propulsive Maneuver Implementation Modes

In order to provide communications with Earth and adequate spacecraft power margin during propulsive maneuvers, the spacecraft –Z axis must be pointed within a specified angle relative to both the Earth and Sun directions. For example, at TCM-1, the angle between the –Z axis and the Earthline direction must be less than 75 deg, and the angle between the –Z axis and the Sunline direction must be less than 50 deg. Consequently, the spacecraft is not free to turn to any arbitrary direction in order to execute TCM-1. The combination of these pointing constraints creates a region within which the spacecraft –Z axis can be pointed. In the discussion that follows, this region is referred to as the "allowable pointing region".

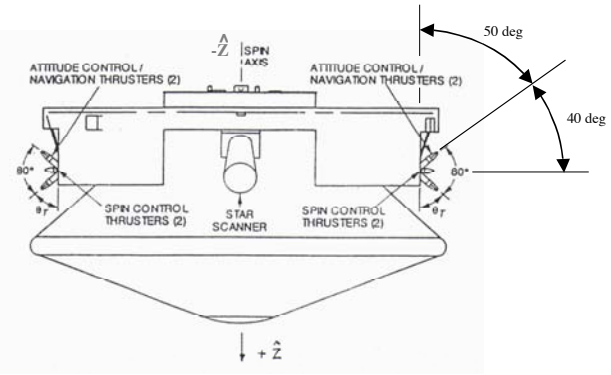

Figure 16: Thruster Cant Angles.

Figure 17 shows the plane defined by the Earthline and Sunline directions, the regions within 75 deg of the Earthline direction (shaded blue) and within 50 deg of the Sunline direction (shaded red), the allowable pointing region (shaded magenta), and maneuver implementation modes for several example ΔV vectors. TA indicates *turn and axial burn*, TL indicates *turn and lateral burn*, and TAL indicates *turn and vector mode burn*. A vector mode burn accomplishes the desired ΔV vector by executing axial and lateral burn components that add to the desired ΔV vector. Performing a vector mode burn without a turn is also an option.

For example ΔV_1, the desired ΔV vector is most efficiently accomplished by a turn and axial burn in the –Z direction. For example ΔV_2, the maneuver is most efficiently accomplished by a turn and lateral burn. For this case, the –Z axis is pointed as indicated by the gray vector in the allowable pointing region. (For simplicity, the lateral ΔV direction is shown perpendicular to the axial ΔV direction.) For example ΔV_3, the maneuver is most efficiently accomplished by a turn and vector mode burn. For this case, the –Z axis is pointed as indicated by the black dashed line labeled "Axial ΔV" on the border of the allowable pointing region.

For statistical maneuver analyses, two options referred to the "MarsVZ" option and "No-Turn Vector" option are considered. The MarsVZ option allows all maneuver implementation modes described above in order to achieve the desired ΔV vector most efficiently: turn and axial burn (TA), turn and lateral burn (TL), and turn and vector mode burn (TAL). The No-Turn Vector option assumes no spacecraft turn is permitted. The spacecraft –Z axis is assumed to be pointed along the nominal cruise attitude direction (which by design satisfies the Earth and Sun pointing constraints).

[**] These assumptions are discussed in more detail in the next section.

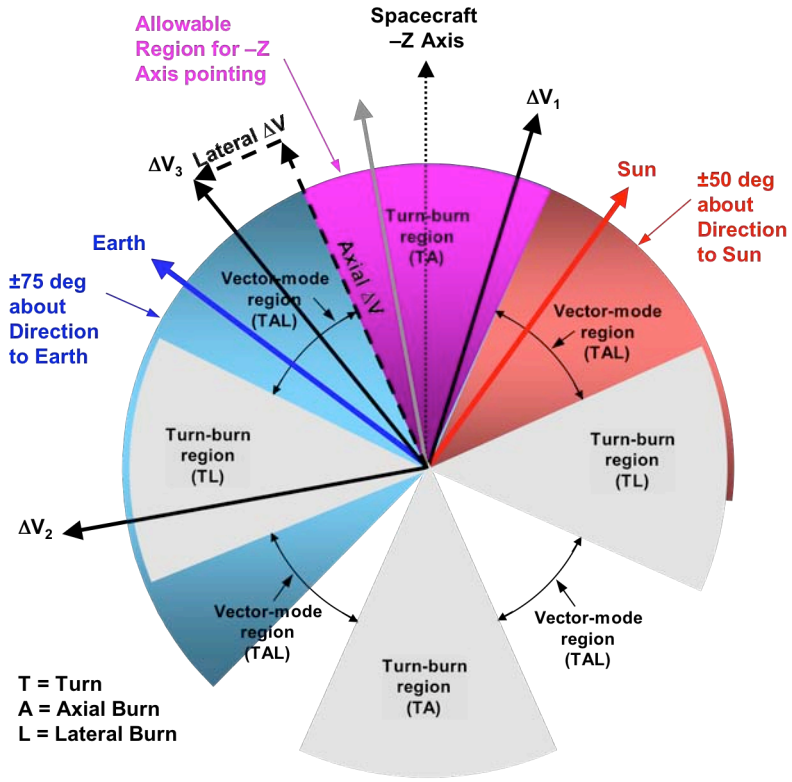

Figure 17: Propulsive Maneuver Implementation Modes.

For TCM-1, the MarsVZ option is used. At the time of TCM-1, the spacecraft is still using the cruise LGA for communications with Earth. The beam width of the LGA permits large off-Earth angles. However, TCMs 2 through 5 are performed after the switch to the cruise MGA. The boresight of the MGA must be pointed within ~9 deg of Earth at all times. For this reason, and for operational simplicity, the No-Turn Vector option is used for all TCMs subsequent to TCM-1.

The physical orientations of the cruise stage thrusters (see Figure 16) cause ΔV penalties for axial and lateral burns. The axial thrusters have a 50 deg cant angle with respect to the axial direction (spacecraft Z axis), and the lateral thrusters have a 40 deg cant angle with respect to the lateral direction (assumed for simplicity to be normal to the axial direction). The cant angle ΔV penalties for axial and lateral burns are:

$$\text{Axial } \Delta V \text{ penalty} = 1/\cos(50°) - 1 = 55.6\%$$
$$\text{Lateral } \Delta V \text{ penalty} = 1/\cos(40°) - 1 = 30.5\%$$

Lateral burns also have a finite burn arc penalty. For lateral burns, the thrusters are fired for 5 s over a burn arc of $\theta = 60$ deg. The finite burn arc penalty is:

$$\text{Lateral burn arc penalty} = (\theta/2)/\sin((\theta/2) - 1 = 4.7\%$$

The overall ΔV penalty for lateral burns is thus 36.7% (1.305 x 1.047 – 1), which is significantly lower than for axial burns (55.6%). From a ΔV penalty standpoint, lateral burns are more efficient. In addition, because the effective Isp of the lateral thrusters is higher, they are even more efficient in terms of propellant mass consumed. This means a lateral burn is often the preferred mode.

Maneuver Execution Accuracy

The accuracy with which a given propulsive maneuver can be executed is a function of the propulsion system behavior and the attitude control system that maintains the pointing of the spacecraft during thruster firings. Propulsion system error sources include thruster misalignments and thrust variations between thrusters. Maneuver execution errors are specified in terms of ΔV magnitude and pointing errors, each of which has a component proportional to the commanded ΔV magnitude (proportional errors) and a component independent of ΔV magnitude ("fixed" errors).

The maneuver execution accuracies for the MSL cruise stage are listed in Table 11. TCM-1 has a higher proportional error, because TCM-1 is the first TCM. The proportional error for subsequent TCMs is lower, because thruster performance will have been calibrated based on results from TCM-1 and from thruster firings

for spacecraft turns and calibration activities. The maneuver execution accuracies in Table 11 are incorporated into statistical maneuver analyses.

Error Source	TCM-1	TCMs 2-5
Proportional magnitude error (3σ)	8%	5%
Proportional pointing error, per axis (3σ)	80 mrad	50 mrad
Fixed magnitude error (3σ)	4 mm/s	4 mm/s
Fixed pointing error, per axis (3σ)	4 mm/s	4 mm/s

Table 11: Maneuver Execution Accuracies.

Injection Aimpoint Biasing

One of the planetary protection requirements listed earlier in this paper states that after injection, the probability of the launch vehicle upper stage (i.e., the Centaur) impacting Mars must be less than 1.0×10^{-4}. In order to meet this requirement, the injection aimpoint must be biased away from Mars. The process to find a biased injection aimpoint that satisfies the above planetary protection requirement and minimizes the subsequent ΔV required to remove the bias determines the point on the 0.7×10^{-4} Mars impact probability ellipse (due to launch vehicle injection errors) in the Mars B-plane, that minimizes the TCM-1 deterministic ΔV. This ellipse is centered on the B-plane aimpoint that corresponds to the atmospheric entry conditions required to achieve the desired landing point. The more conservative value of 0.7×10^{-4} is used to allow for slight inaccuracies from using linearized methods for determining the impact probability.

Note that the method described above provides a biased injection aimpoint that minimizes TCM-1 deterministic ΔV. This aimpoint does not minimize total cruise statistical ΔV when known error sources, such as launch vehicle injection errors, orbit determination errors, and maneuver execution errors, are included. However, given that the process of finding the biased injection aimpoint that minimizes total cruise statistical ΔV would involve a laborious iterative process, and that ΔV and propellant margins are not currently a significant concern (as will be shown in the results that follow), the biased aimpoint has been determined to minimize deterministic TCM-1 ΔV for the analyses contained herein.

Figure 18 shows, for an example case, the 1σ injection error ellipse, the 10^{-4} Mars impact probability ellipse, and the biased injection aimpoint and associated 1σ error ellipse in the Mars B-plane. The size, shape, and orientation 1σ injection error and 10^{-4} Mars impact probability ellipses depend on injection errors and trajectory dynamics. The biased injection aimpoint for the spacecraft is chosen such that the Mars impact probability is $\sim 0.7 \times 10^{-4}$.

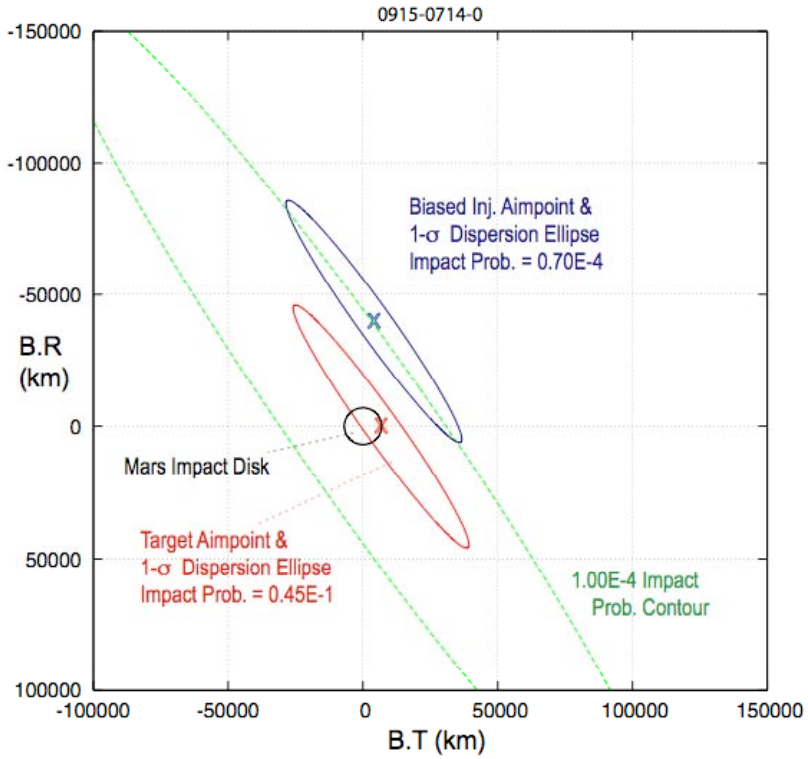

Figure 18: 1σ Injection Error Ellipse, 10^{-4} Mars Impact Probability Ellipse, Biased Injection Aimpoint and Associated 1σ Error Ellipse in Mars B-plane for Launch on 15 September 2009.

Following the injection burn, the Centaur upper stage experiences ΔVs caused by spacecraft separation at injection + 3.7 min, the Contamination and Collision Avoidance Maneuver (CCAM) at injection + ~17 min to move the Centaur away from the spacecraft and preclude contamination of the spacecraft during the subsequent blowdown maneuver, and finally the blowdown maneuver to deplete residual Centaur propellant. The effect on the Centaur trajectory of these ΔVs must be taken into account in satisfying the Centaur impact probability requirement.

The attitudes for spacecraft separation, CCAM, and blowdown determine the direction of the ΔVs experienced by the Centaur for these events. The separation attitude has been determined to ensure that the spacecraft has adequate telecom and power margins for the first 15 days following injection. This attitude is such that the separation ΔV always moves the Centaur aimpoint away from Mars and decreases the Centaur Mars impact probability. The attitudes for CCAM and blowdown may be specified, within launch vehicle attitude constraint, such the ΔVs from these events will also move the Centaur aimpoint away from Mars. A single CCAM attitude has been found that has the desired characteristics, and the blowdown maneuver uses this same attitude.

Non-nominal Impact Probability

The second planetary protection requirement states that the cumulative probability of non-nominal impact of Mars due to spacecraft failure during the cruise phase must be less than 1.0×10^{-2}. A non-nominal impact is an impact that could result in the break-up of the spacecraft and release of terrestrial contaminants on Mars. For TCMs 1 through 4, the non-nominal impact probability is defined as the probability of impact after the TCM, P(i), multiplied by the probability that the subsequent maneuver does not occur, Q(i+1). The Q(i+1) values are supplied by the planetary protection office at JPL and are based on an assumed spacecraft failure rate. For TCM-5 (nominally the final maneuver), the non-nominal impact probability is defined as an impact resulting from a trajectory with an EFPA that violates the ±0.20 deg EFPA delivery requirement, and the associated Q(i+1) value is 1.0. The total non-nominal impact probability is computed as:

$$\Sigma\{ \Pi [1-Q(i)] \times P(i) \times Q(i+1) \}$$

The $\Pi [1-Q(i)]$ term above represents the probability that all preceding maneuvers have been completed successfully and has a value very close to, but slightly smaller than, 1.0. However, this term has not conventionally been included in non-nominal impact probability calculations, so that the slightly more conservative value computed from $\Sigma [P(i) \times Q(i+1)]$ is used. The difference in the resulting cumulative non-nominal impact probability is on the order of 10^{-5}, and, therefore, does not significantly affect the results.

Preliminary calculations have shown that, if all TCMs are targeted directly to the desired atmospheric entry conditions at Mars, the total non-nominal impact probability exceeds the 1.0×10^{-2} requirement. The largest contributions are from TCMs 1, 2, and 3. Consequently, the aimpoints for TCMs 1 and 2 are biased away from Mars (according to empirically determined rules) to reduce their contributions to the total non-nominal impact probability. For TCM-1, the B-magnitude of the aimpoint is constrained to be ~200 km further from Mars than the desired aimpoint. For TCM-2, the B-magnitude is constrained to be further from Mars than the desired aimpoint by an amount corresponding to the semi-major axis dimension of the TCM-2 delivery error ellipse (typically ~700 km). For statistical maneuver analyses, the biased aimpoints for TCMs 1 and 2 are optimized, within the constraints described above, to minimize the total ΔV cost of TCMs 1 through 3.

Table 12 shows an example of a non-nominal impact probability calculation, along with the details of

Event	P(i)	Q(i+1)	P(i) x Q(i+1)	Σ [P(i) x Q(i+1)]
Launch	0.00E+00	2.93E-06	0.00E+00	0.00E+00
Injection	7.00E-05	1.05E-03	7.36E-08	7.36E-08
TCM-1	1.31E-04	3.16E-03	4.15E-07	4.89E-07
TCM-2	2.61E-02	1.27E-02	3.32E-04	3.32E-04
TCM-3	1.00E+00	3.61E-03	3.61E-03	3.94E-03
TCM-4	1.00E+00	4.16E-04	4.16E-04	4.36E-03
TCM-5	2.79E-16	1.00E+00	2.79E-16	4.36E-03

P(i) = non-nominal impact probability following TCM(i)
= total impact probability (with 100 km atmosphere) for TCMs 1 through 4
= impact probability for EFPA violating ±0.20 deg delivery requirement for TCM-5
Q(i+1) = probability that TCM(i+1) does not occur, given that TCM(i) has occurred
TCM-1 aimpoint constraint ⇒ |B| > target + 200 km (i.e., outside impact radius)
TCM-2 aimpoint constraint ⇒ |B| > target + 700 km (1 SMAA of delivery ellipse)

Table 12: Non-nominal Impact Probability for Launch on 15 September 2009.

the TCM-1 and TCM-2 aimpoint constraints. For this case, the total non-nominal impact probability is 4.36×10^{-3}, with the largest contribution from TCM-3.

TCM ΔV and Propellant Statistics

Statistical Maneuver Analysis Process

The statistical maneuver analysis process determines the TCM ΔV and cruise propellant (including ACS propellant) required at the 99% probability level for TCMs and spacecraft attitude/spin control. The TCM ΔV and cruise propellant statistics are generated by performing 5000-sample Monte-Carlo analyses that simulate dispersions caused by launch vehicle injection errors, orbit determination errors, and maneuver execution errors; these analyses also take into account injection and TCM aimpoint biasing for planetary protection and landing site retargeting after launch. For each Monte Carlo sample, the total ΔV for TCMs 1, 2, and 3 is minimized by varying the (biased) aimpoints for TCMs 2 and 3 within the constraints imposed to satisfy the requirement for spacecraft non-nominal impact probability. TCM-3 targets to the final desired atmospheric entry aimpoint. Figure 19 shows, for the same example case as was used for Figure 18, the statistical mean aimpoints and 1s delivery error ellipses for TCMs 1 and 2. The point labeled "Target Aimpoint" corresponds to the desired atmospheric entry aimpoint.

Landing Site Retargeting

Landing site retargeting after launch is also taken into account for statistical maneuver analyses. Landing site retargeting refers to retargeting the interplanetary trajectory to an atmospheric entry aimpoint that corresponds to a different landing site than was used to develop the final launch vehicle injection targets. The final launch vehicle injection targets (C_3, DLA, and RLA) are delivered to the launch services provider at approximately 5 months prior to launch. The work to develop the target specification document starts at about 10 months prior to launch, at which time selection of the final landing site will not yet have occurred. Therefore, the final launch vehicle injection targets are determined from interplanetary trajectories targeted to what is referred to as the "central landing site" (defined below). Following launch, the trajectory is retargeted to the final selected landing site, starting at TCM-1 and using the TCM-1/2/3 optimization process described above.

The central landing site is defined as the landing point with a latitude and longitude each of which is approximately at the midpoint of the extremes of latitude and longitude for all candidate landing sites. This minimizes the maximum latitude and longitude changes required for retargeting the landing site after launch. The Δ V cost for landing site retargeting is

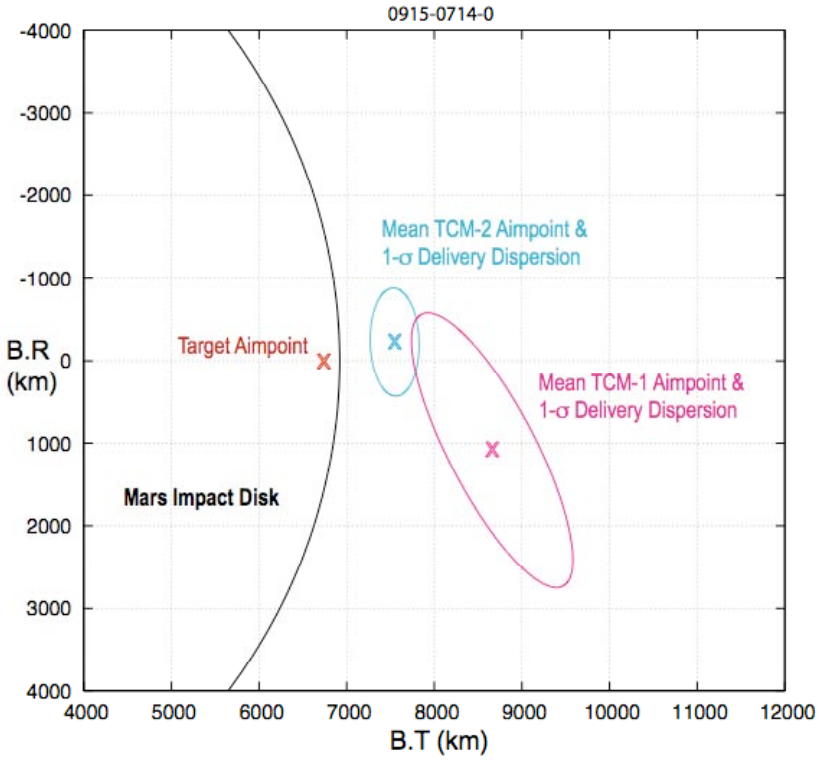

Figure 19: Statistical Mean Aimpoints and 1σ Delivery Error Ellipses for TCMs 1 and 2 for Launch on 15 September 2009.

driven by longitude changes, which require changing the arrival time at Mars; in contrast, the ΔV cost for latitude changes is significantly less. Prior to the addition of the Gale landing site, the minimum and maximum latitudes for all candidate landing sites (see Figure 2) were 26.4S (Holden) and 24.7N (Mawrth). Similarly, the minimum and maximum longitudes were -34.9E (Holden) and 74.5E (Nili). The central landing site was chosen to be at 0.0N / 20.0E, with a maximum required longitude change of ~55 deg. The statistical TCM ΔV and propellant results presented below assume this central landing site. With the Gale landing site (4.5S, 137.4E) included, the central landing site would be at 0.0N / 50.0E, resulting in a maximum required longitude change of ~87 deg. The propellant required to achieve this larger longitude change is also presented below.

Propellant Calculations

In order to calculate statistical cruise propellant mass, first the "ideal" ΔVs for each TCM are computed for each Monte Carlo sample as described above. The ideal ΔV represents the desired inertial velocity change and does not reflect ΔV penalties caused by propulsion system inefficiencies, such as thruster cant angles and the lateral finite burn arc, or ΔV penalties for particular maneuver implementation modes (e.g., vector mode maneuvers) that are required because of spacecraft –Z axis pointing constraints. The ideal ΔVs are then converted to "implemented" ΔVs, which account for all the ΔV penalties mentioned above. The implemented ΔVs are then used to calculate the total cruise propellant mass (via the rocket equation) for each Monte Carlo sample.

Total cruise propellant includes ACS propellant usage in addition to TCM propellant. ACS propellant is required for the activities:

- Spin rate correction after launch vehicle separation.
- Spacecraft turns for TCM-1.
- Attitude/spin maintenance during and after TCMs.
- ACS/NAV characterization turns.
- Attitude maintenance turns.
- Turns to calibrate the descent stage IMU.
- Fault protection response turns.

Mean and 1σ values for the above activities have been supplied by the flight system team. The propellant for TCM-1 turns is a function of the TCM-1 turn angle statistics from the Monte Carlo maneuver analysis. The 99% value for ACS propellant usage is typically 13-14 kg and does not vary significantly as a function of interplanetary trajectory (i.e., launch and arrival dates). The final step is to combine the TCM and ACS propellant statistics to produce total cruise propellant statistics.

Statistical Maneuver Analysis Results

Table 13 lists the eight cases for which statistical maneuver analyses have been performed. These cases correspond to open and close of the baseline and extended launch periods. For each case the landing site is retargeted after launch from the central landing site at 0.0N/20.0E to the Nili and Holden landing sites. Prior to the addition of Gale, these two sites represented the largest combined latitude and longitude changes with respect to the above central landing site.

Launch Period	Launch Date	Arrival Date	Landing Sites*
Baseline	15-Sep-2009	14-Jul-2009	Nili (21.0N, 74.5E) Holden (26.4S, 325.1E)
	14-Oct-2009	1-Aug-2010	
Extended	15-Oct-2009	4-Aug-2010	
	10-Nov-2009	5-Sep-2010	
*Central landing site: 0.0N, 20.0E.			

Table 13: Statistical Maneuver Analysis Cases.

Table 14 presents a summary of the statistical maneuver analysis results for the case at open of the baseline launch period for the Holden landing site, along with key assumptions and constraints. The table includes, for each TCM, the deterministic ΔV (for the reference trajectory) and the mean, 1σ, and 99% values for ideal and implemented ΔV and propellant mass. The total propellant required for TCMs and ACS at the 99% probability level is 37.8 kg, of which 24.5 kg are for TCMs and ~13.3 kg are for ACS. With respect to the 70- kg cruise stage propellant load, the propellant margin is a healthy 32.3 kg (46%). Note that these results are for a central landing site at 0.0N / 20.0E.

Several facts are worth noting with respect to the data in Table 14. The largest part of the deterministic ΔV to remove the launch vehicle injection bias and retarget the landing site occurs at TCM-2. This indicates that it is more efficient from a celestial mechanics standpoint to accomplish these corrections at TCM-2. If the entire deterministic ΔV were forced to occur at TCM-1, the total deterministic ΔV would be significantly higher. Although TCM-2 has by far the larger deterministic ΔV, the 99% values for ideal ΔV, implemented ΔV, and propellant mass are roughly equivalent for TCMs 1 and 2. This indicates that it is more efficient to correct many launch vehicle injection dispersions at TCM-1. The growth factor from ideal ΔV to implemented ΔV is ~1.7, and the conversion factor from implemented ΔV to propellant mass is ~1.9 kg/m/s, which is directly a function of ΔV, spacecraft mass, and I_{sp}. Overall, 1 m/s of ideal ΔV translates into ~3.3 kg of propellant mass.

For the other cases in Table 13, the detailed results show similar behavior to that shown in Table 14, although the numerical values are different. The results for all eight cases are summarized in Table 15. All cases have adequate propellant margin for the landing sites analyzed, assuming a central landing site at

TCM	Location	Det. ΔV (m/s)	Ideal ΔV (m/s)			Implemented ΔV (m/s)			Propellant Mass (kg)		
			μ	1σ	ΔV_{99}	μ	1σ	ΔV_{99}	μ	1σ	ΔM_{99}
TCM-1	L + 15 d	0.31	1.27	0.96	4.05	2.16	1.62	6.92	4.17	3.14	13.32
TCM-2	L + 120 d	2.46	2.44	0.56	3.83	4.12	1.02	6.97	7.82	1.95	13.22
TCM-3	E - 60 d	0	0.29	0.14	0.72	0.55	0.27	1.35	1.06	0.51	2.61
TCM-4	E - 8 d	0	0.08	0.04	0.21	0.15	0.08	0.42	0.29	0.16	0.81
TCM-5	E - 2 d	0	0.02	0.01	0.04	0.03	0.02	0.08	0.06	0.03	0.15
Total		**2.77**	**4.10**	**1.12**	**7.36**	**7.02**	**1.98**	**12.71**	**13.40**	**3.83**	**24.51**

Assumptions and constraints:
- Injection covariance matrix from July 2007 launch trajectory analysis.
- Planetary protection biasing for injection, TCM-1 & TCM-2.
- TCM-1: MarsVZ mode; TCMs 2-5: vector mode.
- TCM-1 turn constraints: 75 deg off-Earth, 50 deg off-Sun.
- Thruster cant angles = 50 deg (axial), 40 deg (lateral).
- Thrust per thruster = 4.7 N.
- Isp = 212.4 s (axial), 221.8 s (lateral).
- Angle between –Z axis and lateral burn direction = 100.6 deg.
- Lateral burn arc = 60 deg (5 s).
- Central landing site = 0.0N / 20.0E.

99% TCM Propellant, kg	=	24.5
ACS Propellant, kg	=	13.3
99% TCM + ACS Propellant, kg	=	37.8
Cruise Propellant Load, kg	=	70.0
Propellant Margin, kg	=	32.2 (46%)

Table 14: Statistical Maneuver Analysis Results: Holden Landing Site, 15 September 2009 Launch, Central Landing Site at 0.0N / 20.0E.

Launch Date	Arrival Date	Landing Site*	Det. ΔV** (m/s)	99% ΔV (m/s)		99% Propellant Mass (kg, %)			
				Ideal	Imple-mented	TCM	TCM + ACS	Margin***	
9/15/09	7/14/10	Holden	2.8	7.4	12.7	24.5	37.8	32.2	46%
		Nili	3.3	7.5	13.0	25.1	38.3	31.7	45%
10/14/09	8/1/10	Holden	4.0	7.5	12.3	23.5	37.5	32.5	46%
		Nili	4.4	8.0	12.7	24.6	38.5	31.5	45%
10/15/09	8/4/10	Holden	3.8	7.3	11.9	22.5	36.4	33.6	48%
		Nili	4.2	8.2	13.3	25.8	39.8	30.2	43%
11/10/09	9/5/10	Holden	4.1	6.8	11.1	21.3	35.7	34.3	49%
		Nili	4.2	7.4	12.0	23.2	37.8	32.2	46%

*Central landing site: 0.0N / 20.0E. **TCM-1 + TCM-2. ***With respect to 70 kg propellant load.

Table 15: Summary of Statistical Maneuver Analysis Results.

0.0N / 20.0E. Note that the total variation in 99% cruise propellant mass and propellant margin across the baseline and extended launch periods is only ~2 kg for both the Holden and Nili landing sites. Also, the values for Holden and Nili are very similar, primarily due to the fact that the longitude changes for retargeting from the central landing site to these landing sites are nearly identical (~55 deg).

The results discussed above assume a central landing site at 0.0N / 20.0E and post-launch retargeting to the Holden and Nili landing sites. This is appropriate if the Gale landing site (added after the analyses discussed above had been completed) is not considered. With Gale included, the central landing site should be at 0.0N / 50.0E, and the maximum required longitude change increases to ~87 deg. In order to understand the ΔV and propellant costs with Gale included, a special study was carried out.

Statistical maneuver analyses have been performed to determine the 99% cruise propellant mass (TCM plus ACS) for longitude changes up to ±180 deg. This longitude range was chosen to encompass the ~87 deg longitude change required for Gale and also to determine the maximum possible longitude change in the event that some new candidate landing site was added in the future. In addition, large latitude changes were included, so that any synergistic effect from a combination of large latitude and longitude changes would be uncovered. These analyses were done for the open of the baseline launch period.

The results are presented in Table 16 In order to reduce the time and effort to generate the results, the old central landing site (0.0N / 20.0E) was used for the

Latitude / Longitude	26.4S / 200.0E	26.4S / 260.0E	26.4S / 325.1E	0.0N / 20.0E	21.0N / 74.5E	21.0N / 140.0E	21.0N / 200.0E
ΔLat / ΔLon (deg)	-26.4 / -180.0	-26.4 / -120.0	-26.4 / -54.9	0 / 0	+21.0 / +54.5	+21.0 / +120.0	+21.0 / +180.0
Entry Date/Time (ET)	7/14/10 21:44	7/14/10 17:37	7/14/10 13:16	7/14/10 9:11	7/14/10 5:35	7/14/10 1:06	7/13/10 21:00
Δ Entry Time	12:32	8:25	4:04	0	-3:36	-8:05	-12:11
Det. ΔV (m/s)*	6.5	4.4	2.8	–	3.3	5.8	8.0
99% Prop. Mass (kg)	58.2	46.0	37.8	–	38.3	47.8	56.8
Prop. Margin (kg)**	11.8	24.0	32.2	–	31.7	22.2	13.2
*TCM-1 + TCM-2. **With respect to 70 kg propellant load.							

Table 16: Cruise Propellant Margin as Function of Longitude Change for Launch on 15 September 2009.

reference for retargeting; however, the results should apply for any central landing site. For each case, the following parameters are tabulated: atmospheric entry date/time, change in entry time, deterministic ΔV, 99% cruise propellant mass (TCM plus ACS), and propellant margin. Note the values for longitude change and propellant margin, which are tabulated in red. These results indicate that for a 70 kg propellant load, any longitude within ±180 deg of the central landing site, for latitudes between about 30N and 30S, can be achieved with retargeting the trajectory after launch. In other words, any point on the surface of Mars with a latitude between about 30N and 30S is accessible.

The two cases in Table 16 for longitude changes of –54.9 deg and +54.5 deg correspond to retargeting to the Holden and Nili landing sites from the old central landing site. The ΔV/propellant results for these two cases are identical to those in Table 15. For the new central landing site, the longitude change required for Holden is –84.9 deg; similarly, the longitude change for Gale is +87.4 deg. These landing sites represent the new bounding cases in terms of maximum required longitude change and maximum propellant usage. By interpolating the data in Table 16, the propellant margins for retargeting to Holden and Gale are estimated to be 28.5 kg and 27.0 kg. These margins are slightly smaller than those in Table 15 because of the larger longitude changes.

EDL TRAJECTORY ANALYSIS

EDL trajectory analysis utilizes software that simulates the EDL trajectory starting at atmospheric entry (or earlier, if necessary) and extending though landing. This trajectory simulation includes all the key EDL events, such as atmospheric deceleration, hypersonic entry guidance, supersonic parachute deployment, powered descent, and landing. The simulation can be performed either in three-degree-of-freedom (3DOF) mode or 6DOF mode and includes EDL guidance, navigation, and control (GNC) flight software as well as flight hardware device models. GNC flight software functionalities include state estimation (position, velocity, attitude, attitude rate), attitude control, entry guidance, and powered descent guidance and control. Flight hardware device models include the entry vehicle ACS thrusters and the descent stage IMU.

The two primary functions for EDL trajectory analysis are reference trajectory design to determine the atmospheric entry aimpoint to achieve a specified landing point and Monte Carlo analyses to evaluate EDL performance, including landing dispersions.

Reference Trajectory Design

The atmospheric entry aimpoint used as the target for interplanetary cruise TCMs consists of inertial EFPA, entry B-plane angle, and entry time, where the entry interface point is defined to be at a Mars radius of 3522.2 km. The nominal value for EFPA is –15.5 deg; however, the EFPA may be adjusted to optimize entry guidance performance.

The design of the reference EDL trajectory involves determination of the entry B-plane and time that achieve a desired landing point (i.e., latitude and longitude) on the surface of Mars, given a specified EFPA and entry guidance profile (specifically, the bank angle profile used to orient the lift vector to null out entry trajectory errors and compensate for atmospheric and aerodynamic dispersions.) Entry B-plane angle and entry time both affect the latitude and longitude of the landing point. The entry B-plane angle and time are varied interactively to converge the latitude and longitude to the desired values. The reference trajectory design may also include an outer-loop to adjust the EFPA to provide desirable characteristics for the entry guidance profile.

Reference EDL trajectories are needed for interplanetary trajectory design (including generation of launch vehicle injection targets), approach navigation analyses (for entry delivery and knowledge accuracies), and cruise statistical maneuver analyses.

Monte Carlo Analyses

EDL Monte Carlo analyses are performed to evaluate EDL system performance in the presence of various error sources. The metrics for EDL system

performance include landing accuracy (i.e., distance from target landing point), aerodynamic heating rate and total heating load, atmospheric entry deceleration level, various parachute deployment parameters (including altitude), and heatshield Mach number. The error sources include atmospheric entry delivery and knowledge errors, entry attitude errors, aerodynamic dispersions, and atmospheric dispersions. The entry delivery and knowledge errors are each represented by a set of 8000 dispersed entry state vectors generated from an approach navigation covariance analysis as described earlier in this paper.

The flight software entry guidance algorithm uses knowledge of the entry state vector (uplinked from the ground), the spacecraft attitude at entry (determined onboard), and sensed accelerations (from the IMU) to "fly out" errors in the entry conditions, compensate for aerodynamic and atmospheric dispersions, and land at the desired point on the surface. This is accomplished by controlling the lift vector of the entry vehicle to adjust crosstrack and downtrack range from the target.

Figure 20 shows an example plot of landing dispersions from an EDL Monte Carlo analysis. These results are for the Mawrth landing site for launch at open of the baseline launch period. DSENDS and POST are the names of EDL trajectory simulation software tools used at JPL and the NASA Langley Research Center. The 99.87% high range error at landing (i.e., distance from target) is 11.9 km[††]. At 99.0% probability, this value is 9.8 km. As compared to MER, the distribution of landing dispersions for MSL is more nearly circular and less Gaussian, and the errors are smaller. The semi-major axis of the MER landing dispersion ellipses (i.e., along the downtrack direction) was typically 30-35 km at the 99% probability level. The more nearly circular shape and non-Gaussian characteristics of the MSL landing dispersions as well as the improved accuracy, all derive from the use of hypersonic entry guidance.

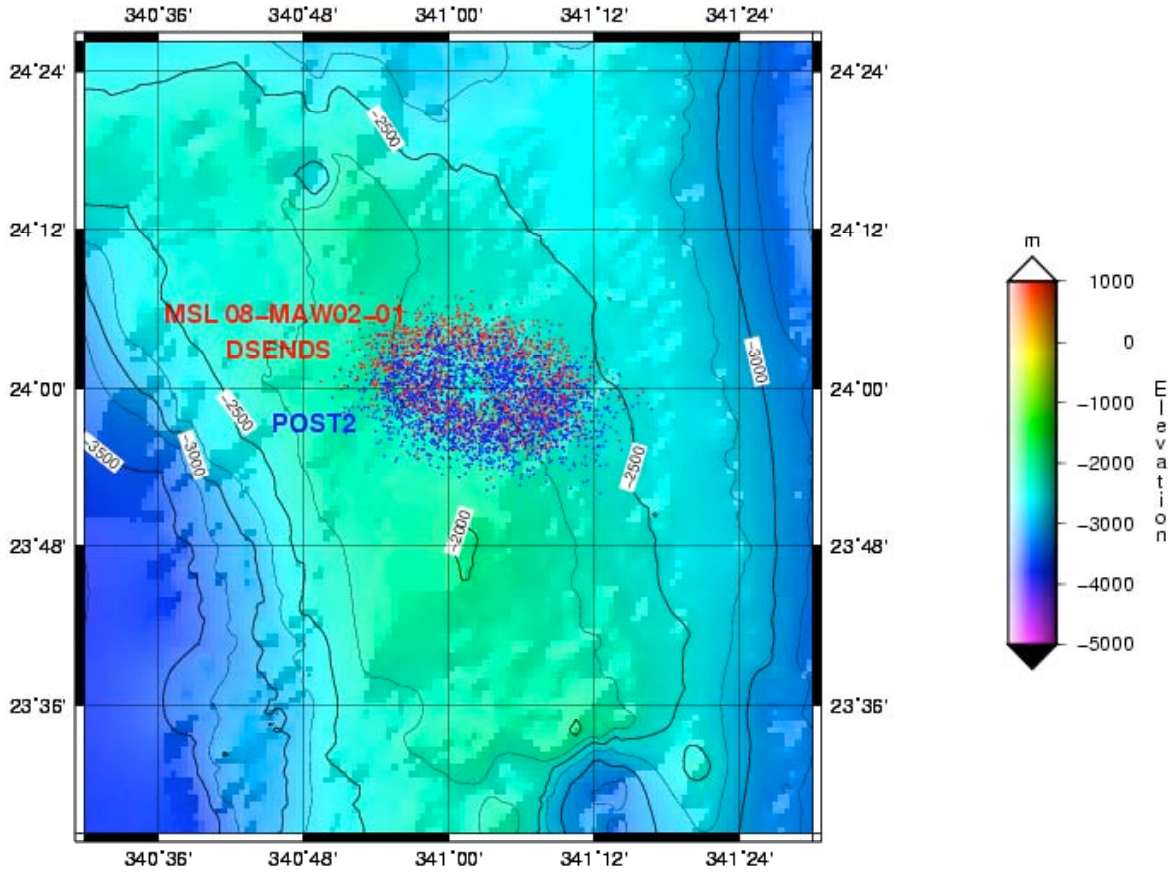

Figure 20: Landing Dispersions from EDL Monte Carlo Analysis 08-MAW02-01: Mawrth Landing Site, 15 September 2009 Launch.

[††] EDL Monte Carlo analyses conventionally report values at the 99.87% probability level, which is the 3σ probability for a one-dimensional normal distribution.

CONCLUSIONS

This paper has described the strategies for mission and navigation design and presented analysis results to demonstrate that all mission and navigation design requirements can be achieved. The launch/arrival strategy provides EDL communications coverage via an X-band DTE link and a UHF link to MRO and ODY for landing latitudes between 30N and 30S. The launch/arrival strategy employs a 30-day baseline launch period and a 27-day extended launch period with varying arrival dates at Mars. The LMST node for the orbit of MRO or ODY must be moved progressively earlier in the extended launch period in order to provide EDL coverage. The navigation strategy makes use of complimentary radiometric data types (Doppler, range, and ΔDOR) for orbit determination and five planned interplanetary TCMs to achieve atmospheric entry delivery and knowledge requirements. A central landing site is used for generation of launch vehicle injection targets, and the trajectory is retargeted to the desired landing site after launch. Statistical maneuver analyses indicate that ample margins exist for required cruise propellant (for TCMs and ACS) with respect to the usable propellant load.

ACKNOWLEDGEMENTS

The research described in this paper was carried out at the Jet Propulsion Laboratory, California Institute of Technology, under a contract with the National Aeronautics and Space Administration.

The author would like to acknowledge the members of the MSL Mission Design and Navigation Team, who performed the analyses that are reported on in this paper: Fernando Abilleira, Darren Baird, Dan Burkhart, Julie Kangas, Tomas Martin-Mur, Sumita Nandi, and Mau Wong. The author also acknowledges the contributions of the MSL EDL systems and GNC teams. Stacy Weinstein, Tim McElrath, and Mike Watkins served as reviewers for this paper and provided useful comments.

REFERENCES

1 Mars Science Laboratory Mission Plan, JPL D-27162, MSL-272-0211, 10 September 2007.

2 Mars Science Laboratory Interplanetary Trajectory Characteristics Document, JPL D-27210, 31 July 2008.

3 Mars Science Laboratory Navigation Plan, JPL D-33445, 7 March 2008.